RANDOLPH, M. F., CARTER, J. P. & WROTH, C. P. (1979). *Géotechnique* **29**, No. 4, 361–393

Driven piles in clay—the effects of installation and subsequent consolidation

M. F. RANDOLPH,* J. P. CARTER* and C. P. WROTH*

This paper describes the results of numerical analysis of the effects of installing a driven pile. The geometry of the problem has been simplified by the assumption of plane strain conditions in addition to axial symmetry. Pile installation has been modelled as the undrained expansion of a cylindrical cavity. The excess pore pressures generated in this process have subsequently been assumed to dissipate by means of outward radial flow of pore water. The consolidation of the soil has been studied using a work-hardening elasto-plastic soil model which has the unique feature of allowing the strength of the soil to change as the water content changes. Thus it is possible to calculate the new intrinsic soil strength at any stage during consolidation. In particular the long-term shaft capacity of a driven pile may be estimated from the final effective stress state and intrinsic strength of the soil adjacent to the pile. A parametric study has been made of the effect of the past consolidation history of the soil on the stress changes due to installation of the pile. The results indicate that for any initial value of overconsolidation ratio, the final stress state adjacent to the pile is similar to that in a normally one-dimensionally consolidated soil except that the radial stress is the major principal stress. A method is described whereby the model of pile installation and subsequent consolidation may be extended to clays which are sensitive. The method is used to predict changes in the strength and water content of soil adjacent to a driven pile which compare well with measurements from two field tests on driven piles. It is also shown that the rate of increase of bearing capacity of a driven pile may be estimated with reasonable accuracy from the rate of increase in shear strength of the soil predicted from the analysis.

Cet article fait part des résultats d'analyses numériques des effets occasionnés par la mise en place d'un pieu battu. L'hypothèse de conditions de déformation plane en plus d'une symétrie axiale a été adoptée pour simplifier la géométrie du problème. Le battage du pieu a été représenté par l'expansion non drainée d'une cavité cylindrique. On a supposé par la suite que les surpressions interstitielles engendrées au cours de ce processus se dissipaient en raison de l'écoulement radial vers l'extérieur de l'eau interstitielle. L'étude de la consolidation du sol a fait appel à un modèle de sol élasto-plastique rigide, qui a pour propriété unique de permettre des modifications de la résistance du sol en fonction des variations de la teneur en eau. Grâce à cela, il est possible de calculer la nouvelle résistance intrinsèque du sol à une étape quelconque de la consolidation. Notamment, il est possible d'estimer le frottement latiére à long terme d'un pieu battu à partir de l'état de contrainte efficace finale et de la résistance intrinsèque du sol adjacent au pieu. L'effet de l'historique de consolidation antérieure du sol sur les variations de contraintes dues à l'installation du pieu a fait l'objet d'une étude paramétrique. Les résultats montrent que pour toute valeur initiale du degré de surconsolidation, l'état de contrainte final au voisinage du pieu est identique à celui d'un sol à consolidation unidimensionnelle normale sauf que la contrainte radiale constitue la contrainte principale majeure. L'article décrit une méthode suivant laquelle le modèle d'installation de pieux et de consolidation subséquente peut être appliqué aux argiles qui sont sensibles au remaniement. La méthode sert à prévoir les variations de la résistance et de la teneur en eau du sol adjacent à un pieu battu, lesquelles sont tres voisines des mesures provenant de deux essais in situ de pieux battus. Il apparaît également que le taux d'accroissement de la capacité portante d'un pieu battu peut etre estimé dans des limites de précision raisonnables à partir du taux d'accroissement de la résistance à la rupture au cisaillement du sol prévu par l'analyse.

INTRODUCTION

Estimation of the shaft capacity of piles driven into clay is an important problem in geotechnical engineering. Until recently, such estimates were generally based on the undrained shear strength of the undisturbed soil, i.e. prior to installing the pile. A factor α was introduced

Discussion on this Paper closes 1 March, 1980. For further details see inside back cover.

* University Engineering Department, Cambridge.

in order to take some account of the disturbance caused by driving the pile. Choice of a suitable value for α relied heavily on the engineer's personal experience, although attempts have been made to correlate α empirically with the strength of the soil (Tomlinson, 1957; McClelland, 1972) or more correctly, with the past stress history of the soil (Wroth, 1972). In the past few years, several workers have endeavoured to interpret the maximum shaft friction on the pile, in terms of the effective stresses acting in the soil around the pile (Chandler, 1968; Burland, 1973; Meyerhof, 1976; Parry and Swain, 1977a and 1977b). The major obstacle to the wider use of effective stress methods of design is lack of knowledge of the effective stress state around the pile. Instruments have been developed for measuring the in situ lateral stresses in the ground (e.g. Wroth and Hughes, 1973) but the problem still remains as to how these stresses are affected by installation of the pile.

When a solid pile is driven into soil, it must initially displace a volume of soil equal to the volume of the pile. At small penetrations, up to about ten times the radius of the pile, some heave of the ground surface occurs (Cooke and Price, 1973). At greater depths, the soil is displaced predominantly outwards in the radial direction. This has led to the installation process being modelled as the expansion of a cylindrical cavity with a final radius equal to that of the pile (Soderberg, 1962; Butterfield and Banerjee, 1970).

There is widespread experimental evidence showing that the bearing capacity of a pile driven into clay increases with time after driving (e.g. Seed and Reese, 1955; Eide, Hutchinson and Landva, 1961). The increase in capacity is largely attributable to the change of water content (and thus of strength) of the clay around the pile as the excess pore pressures generated during installation dissipate. This process of consolidation may occupy several months, depending on the diameter of the pile and the coefficient of consolidation of the soil.

Analyses of the stress changes due to the expansion of a cylindrical cavity and the subsequent consolidation of the soil have been presented by Carter, Randolph and Wroth (1979) and Randolph and Wroth (1979) for soil idealized as an elastic or elastic, perfectly plastic material. The former paper also gave preliminary results for the case of a soil modelled as a work-hardening elasto–plastic material, based on modified Cam-clay (Roscoe and Burland, 1968). In this Paper these preliminary results are extended to include an investigation of the effect of the past stress history of the soil on the stress changes due to pile installation. Simple rules are presented for estimating the excess pore pressures set up during pile driving and for the times necessary for these pore pressures to dissipate. It is shown that, whatever the initial value of overconsolidation ratio (OCR), the soil close to the pile ends up as one dimensionally normally consolidated with the radial stress as the major principal stress.

At the end of the Paper, measurements of the variation in bearing capacity with time of two driven piles are interpreted in the light of the theoretical analyses. It is shown that accurate predictions may be made of the changes with time of the strength and water content of the soil adjacent to a driven pile.

THE WORK-HARDENING SOIL MODEL

The results presented later in this Paper were obtained using a volumetric work-hardening soil model. The model is based on the critical state concepts (Schofield and Wroth, 1968) and is similar to the model suggested by Roscoe and Burland (1968). It is capable of predicting quantitatively many of the observed features of normally consolidated and lightly overconsolidated clays and has been used in predictions of real boundary value problems with encouraging success (e.g. Wroth and Simpson, 1972; Naylor, 1975; Wroth, 1977). Details of its formulation, suitable for use in finite element calculations, can be found in several sources

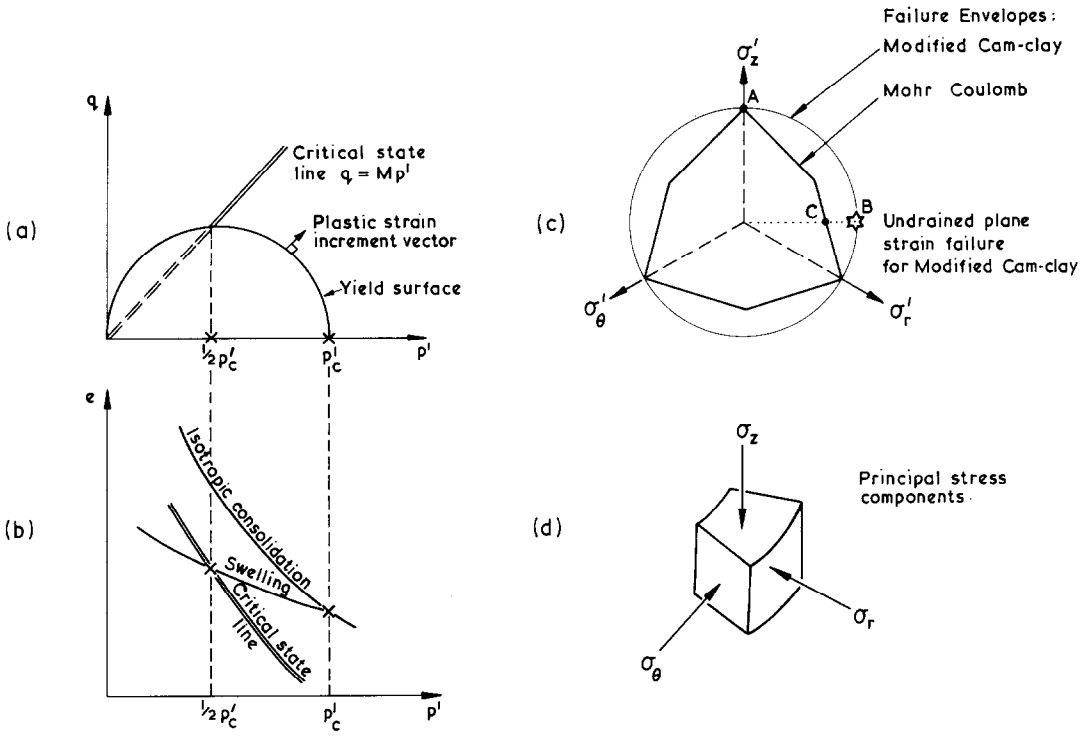

Fig. 1. Essential features of the work-hardening soil model

(e.g. Zienkiewicz and Naylor, 1971). The key features of the model are illustrated in Fig. 1.

This material (so called modified Cam-clay) requires the specification of five parameters and values for all of them may be obtained from standard laboratory tests. These parameters are

- λ the gradient of the virgin consolidation line in e–ln p' space
- κ the mean gradient of the swelling and re-compression line in e–ln p' space
- e_{cs} the value of e at unit p' on the critical state line in e–ln p' space
- M the value of the stress ratio q/p' at the critical state condition
- G the elastic shear modulus

In this notation e refers to the current voids ratio of the soil while the quantities p' and q are given by

$$p' = \tfrac{1}{3}(\sigma_r' + \sigma_\theta' + \sigma_z') \quad . \quad . \quad . \quad . \quad . \quad . \quad . \quad . \quad . \quad (1)$$

$$|q| = \sqrt{[\tfrac{1}{2}\{(\sigma_r' - \sigma_\theta')^2 + (\sigma_\theta' - \sigma_z')^2 + (\sigma_z' - \sigma_r')^2\}]} \quad . \quad . \quad . \quad . \quad (2)$$

The relationship between the parameter[1] q and the octahedral shear stress τ_{oct} is given by

$$q = (3/\sqrt{2})\,\tau_{oct} \quad . \quad . \quad . \quad . \quad . \quad . \quad . \quad . \quad . \quad . \quad (3)$$

In addition to these parameters a full description of the material requires specification of the soil permeability k, the unit weight of the pore fluid γ_w and a knowledge of the in situ stresses at each point in the soil.

[1] The definition of q is such that it reduces to the deviator stress when two of the principal stresses are equal, as is the case for a conventional triaxial test.

Table 1. Details of numerical computations, Boston Blue clay

$\lambda = 0{\cdot}15$, $\kappa = 0{\cdot}03$, $e_{cs} = 1{\cdot}744$, $M = 1{\cdot}2$

Case	OCR	K_0	G/c_u	$G/\sigma_z'(0)$	$G/p'(0)$
A	1	0·55	74	25	36
B	2	0·7	83	50	63
C	4	1·0	91	101	100
D	8	1·35	100	201	164
E	32	2·75	118	806	372
F	8	1·35	22	44	36

For stress states within the yield surface the deformations are determined by the elastic bulk modulus K and the shear modulus G. In this model $K = (1+e)p'/K$, i.e. K is stress dependent, but G is held constant, and so the model is conservative for elastic behaviour (see Zytynski *et al.*, 1968). Yielding occurs whenever the stresses obey the following criterion

$$q^2 - M^2\{p'(p_c' - p')\} = 0 \quad . \quad . \quad . \quad . \quad . \quad . \quad . \quad . \quad . \quad (4)$$

where p_c' is a hardening parameter given by the intersection of the current ellipsoidal yield locus and the p' axis in principal effective stress space. As the material yields and hardens, plastic flow is determined by an associated flow rule.

PARAMETRIC STUDIES

In order to be specific, a set of soil parameters was chosen so that the work hardening model would simulate a deposit of soil like Boston Blue clay. The numerical values of these parameters are given at the head of Table 1. Values have not been quoted for k or γ_w since these parameters only affect the rate of pore pressure dissipation and thus will only appear in the non-dimensionalized time parameter. This soil was considered to be initially one dimensionally consolidated in the field with a value of $K_0 = 0{\cdot}55$ and then allowed to swell back after removal of overburden stress. A number of different starting conditions was assumed just prior to pile installation. Each case corresponds to an overconsolidation ratio (defined in the conventional way as the ratio of past maximum effective vertical stress σ_{zm}' to the in situ vertical effective stress $\sigma_z'(0)$, i.e. OCR $= \sigma_{zm}'/\sigma_z'(0)$), OCR = 1, 2, 4, 8 or 32 (cases A to E of Table 1). Case F is discussed later. For every soil examined the voids ratio before cavity expansion was 1·16. The choice of a unique value of initial voids ratio was made so that all soils would have the same initial undrained shear strength for ease of comparison.

It should be made clear that the undrained shear strength quoted in this Paper is the value relevant to conditions of plane strain and represents the strength of the soil in situ, prior to pile driving. Since the modified Cam-clay yield locus is a surface of revolution about the p' axis in stress space, the value of undrained shear strength (defined as $c_u = \frac{1}{2}(\sigma_1' - \sigma_3')$) will depend on the value of the intermediate principal stress σ_2'. In contrast to this, q_f, the value of q at failure, will remain constant no matter what type of loading is carried out. Figure 1(c) shows the intersection of the Modified Cam-clay failure (or critical state) surface with the π plane in principal stress space. For comparison a typical Mohr–Coulomb failure envelope is also shown. In a conventional triaxial test $\sigma_2' = \sigma_3'$ and so the undrained shear strength is given by $c_u = \frac{1}{2}(\sigma_1' - \sigma_3') = q_f/2$. In undrained plane strain conditions the intermediate principal stress will be equal to the average of the major and minor principal stresses and thus $c_u = \frac{1}{2}(\sigma_1' - \sigma_3') = q_f/\sqrt{3}$.

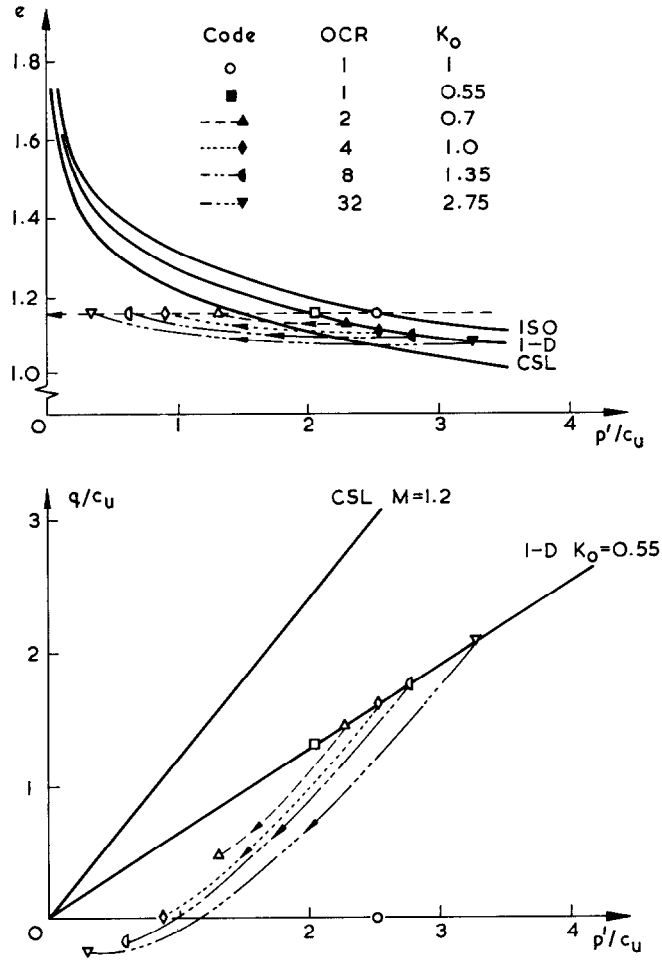

Fig. 2. Consolidation histories and in situ stress conditions before pile driving

The history of each of the soil samples up to the beginning of pile driving (cavity expansion) is depicted in Fig. 2 and the values of OCR, K_0 and G for each are tabulated in Table 1. In clay soils there is a link between the current value of overconsolidation ratio during monotonic unloading and the current value of K_0. The values for K_0 quoted in Table 1 were calculated using the relationship suggested by Wroth (1975). The choice of a suitable value for the elastic shear modulus G at different values of OCR is more difficult and requires some comment. Clearly in most soils it would be wrong to associate G with the current in situ stress state since this would result in low, unrealistic values of G, hence low values of the ratio G/c_u, at high values of OCR (Zytynski *et al.*, 1978). A more rational approach would be to select G as some fixed proportion of the maximum value of the elastic bulk modulus, K_{max} that was ever reached during the history of the soil. The value of K_{max} is given by

$$K_{max} = \frac{1+e_{min}}{\kappa} p_{max}' \quad . \quad . \quad . \quad . \quad . \quad . \quad . \quad . \quad . \quad . \quad (5)$$

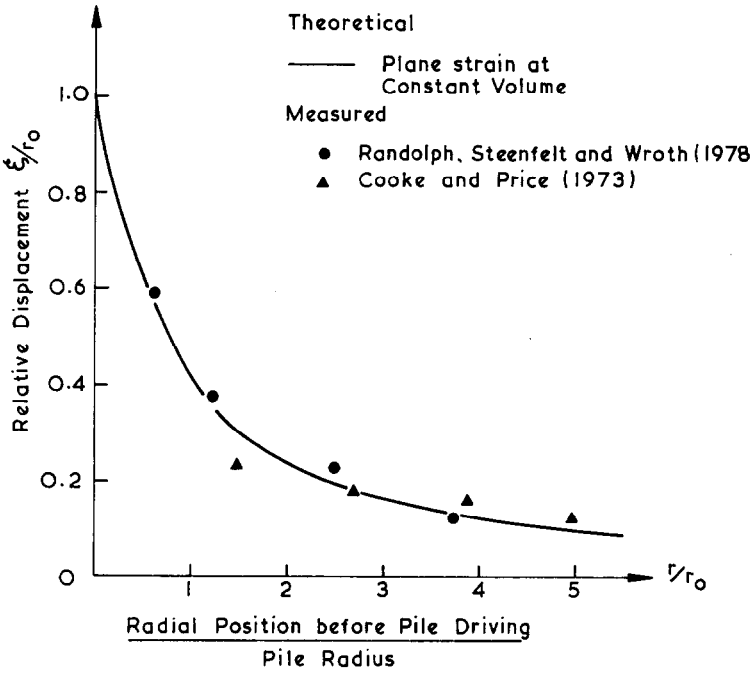

Fig. 3. Comparison of measured and theoretical soil displacements

where p_{max}' is the maximum past value of p', and e_{min} is the corresponding minimum past voids ratio. The proportional relation adopted is

$$G = 0{\cdot}5K_{max} \quad . \quad . \quad . \quad . \quad . \quad . \quad . \quad . \quad . \quad . \quad . \quad (6)$$

This choice of indirect connection between OCR and G means that the ratios $G/\sigma_z'(0)$ and $G/p'(0)$ increase with OCR (where $\sigma_z'(0)$ and $p'(0)$ are the initial, in situ values of σ_z' and p' respectively) a feature that is consistent with observations of many clays.[2] It also implies that an overconsolidated soil is stiffer in shear than a soil which is normally consolidated to the same effective overburden pressure. The sensitivity of the stress changes caused by pile driving to the selection of a value for G is discussed later.

The suitability of modified Cam-clay for modelling the behaviour of heavily overconsolidated clays has been questioned (Parry and Amerasinghe, 1973; Banerjee and Stipho, 1979). The criticisms are mainly levelled at the value of the predicted soil strength at high values of OCR. In order to avoid this difficulty, the results presented in this Paper are normalized in terms of the initial undrained shear strength of the soil (and not in terms of the initial vertical effective stress and the value of OCR). In general, the main features of the behaviour of heavily overconsolidated clay are preserved by the model (for instance the large pseudo-elastic range of the soil and the tendency of the mean effective stress to increase near failure as the soil is sheared under undrained conditions).

ANALYSIS OF THE INSTALLATION OF THE PILE

When a pile is driven into the soil, there is a region around the tip of the pile where extensive

[2] In particular, reference is made to a series of high quality laboratory tests on carefully trimmed specimens from blocks of London clay tested at Imperial College, London, by Webb (1967) and interpreted by Wroth (1971).

disturbance and remoulding of the soil takes place. Studies of the displacement pattern in this region have shown the displacements to be midway between those associated with the expansion of a spherical cavity and those associated with the expansion of a cylindrical cavity (Clark and Meyerhof, 1972; Roy *et al.*, 1975). Model studies have also shown that little further vertical movement of soil occurs at any level once the tip of the pile has passed that level (Randolph, Steenfelt and Wroth, 1979). Immediately after installation, when the jacking or driving force has been removed, the average shear stress down the pile shaft is likely to be small (merely balancing any residual force on the pile base).

Measurements of the radial movement of soil near the pile mid-depth taken from the model tests of Randolph, Steenfelt and Wroth (1979), together with some field measurements of Cooke and Price (1973) have been plotted in Fig. 3. The radial displacement of the soil during pile driving has been plotted against radial position before driving. Both sets of measured results agree well with the theoretical prediction made on the assumption of plane strain, cylindrical deformation at constant volume.

From the above considerations, it is reasonable to expect that the stress changes in the soil over much of the length of the pile shaft (ignoring the regions close to the ground surface and to the pile tip) will be similar to those produced by the expansion of a cylindrical cavity. In the first instance, the residual shear stresses on the interface between the pile and soil will be ignored.

With these assumptions, it may be shown (Hill, 1950; Carter *et al.*, 1979; Randolph and Wroth, 1979) that the installation of a pile into a soil modelled as an elastic perfectly plastic material, causes excess pore pressures (equal to the increase in mean total stress) to be generated given by

$$u = 2c_u \ln(R/r), \quad r_0 \leqslant r \leqslant R$$

where

$$R^2 = (G/c_u)\, r_0^2 \qquad (7)$$

In particular, the maximum excess pore pressure at the pile face is

$$u_{max} = c_u \ln(G/c_u) \qquad (8)$$

While the elastic perfectly plastic soil model has the advantage that a closed-form solution is possible for the cavity expansion problem, the model has two important short-comings. Firstly, no account is taken of pore pressure generated due to pure shear—i.e. with no change in mean total stress. This can be remedied to some extent by the use of a pore pressure parameter to estimate the excess pore pressure due to deviatoric stress change. However, such a soil model will still lead to incorrect relative magnitudes of the three principal stresses compared with a more sophisticated, elasto–plastic model which takes account of the plastic strains which occur in soil even at low stress levels. The second shortcoming is the inability of the elastic perfectly plastic soil model to link correctly the strength of the soil and its change with the current effective stress state and stress history of the soil.

To overcome these shortcomings, the modified Cam-clay soil model described previously has been used, by means of the finite element method, to analyse the stress and pore pressure changes due to cavity expansion. The process of modelling the creation of a cylindrical cavity has been described by Carter *et al.* (1979) and is achieved within sufficient accuracy by doubling the radius of a cavity initially at radius a_0. The strain field in the soil around a driven pile of radius r_0 is matched if a_0 is chosen to be $r_0/\sqrt{3}$ (see Carter *et al.*, 1979). The solutions for soil initially at states A to E in Table 1 are given in Figs 4 to 8. It should be noted that ambient pore pressures have not been included in any plots of total stress.

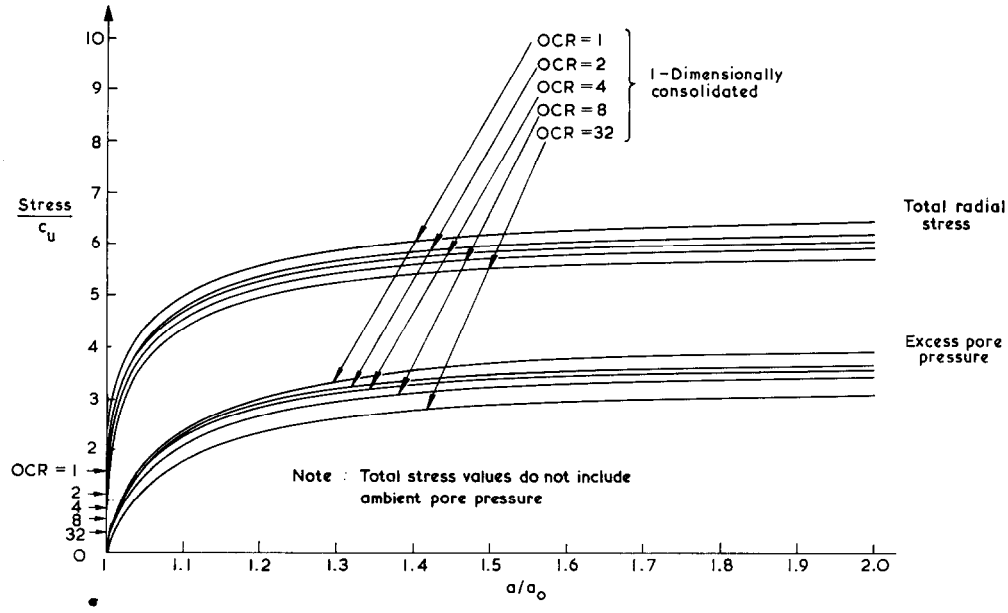

Fig. 4. Total radial pressure and excess pore pressure generated close to the pile (at $r = 1{\cdot}15\,r_0$) during cavity expansion

Figure 4 shows plots of total radial stress σ_r and excess pore pressure u at the cylindrical cavity surface, as functions of the cavity radius a. In all cases, σ_r and u have approached limiting values by the time that the cavity has doubled in size. Of particular importance is the observation that the ratio of these limiting values to the initial undrained shear strength c_u of the soil is almost independent of the one dimensional consolidation history needed to achieve the value of c_u; that is the undrained shearing which is caused by pile installation has effectively erased the memory of the soil close to the pile. This feature is reflected in Fig. 5(a) which shows a plot of excess pore pressure (normalized by c_u) generated close to the pile during driving as a function of OCR. Only a small decrease is observed at higher values of OCR. An alternative method of presenting this result is shown in Fig. 5(b) where the pore pressure has been normalized by $\sigma_z'(0)$, the effective overburden stress in the soil prior to driving. As expected, this plot shows a steep increase with OCR in the predicted value of $u/\sigma_z'(0)$.

Stress distributions at the end of cavity expansion are shown in Figs 6 and 7 for soils with OCR = 1 and 8. The effect of the choice of the elastic shear modulus G is shown in Fig. 7 for OCR = 8 where two different values of G were used, one being proportional to the past maximum, and one to the present mean effective stress; the ratio of the values for G is $100/22 \simeq 4{\cdot}5$. The undrained shear strength and all other model parameters were the same for both soils (cases D and F of Table 1). The soil with the larger elastic shear modulus develops higher excess pore pressures and limiting pressure σ_r. From Fig. 7 it may be seen that the effective stresses are the same in the failed region of soil for the two different values of G; this is a consequence of the undrained strengths being the same in each case. The effect of the differences in total stress changes during cavity expansion in the final effective stress distribution after consolidation, is discussed later in the Paper.

It may be noted from Fig. 7 that there is a zone of tensile circumferential stress for $6 \leqslant r/r_0 \leqslant 10$–11. This is a feature of the analyses for OCR > 8 and it has been assumed in the Cam-clay model that the soil will sustain these tensile stresses. In reality, however, cracks

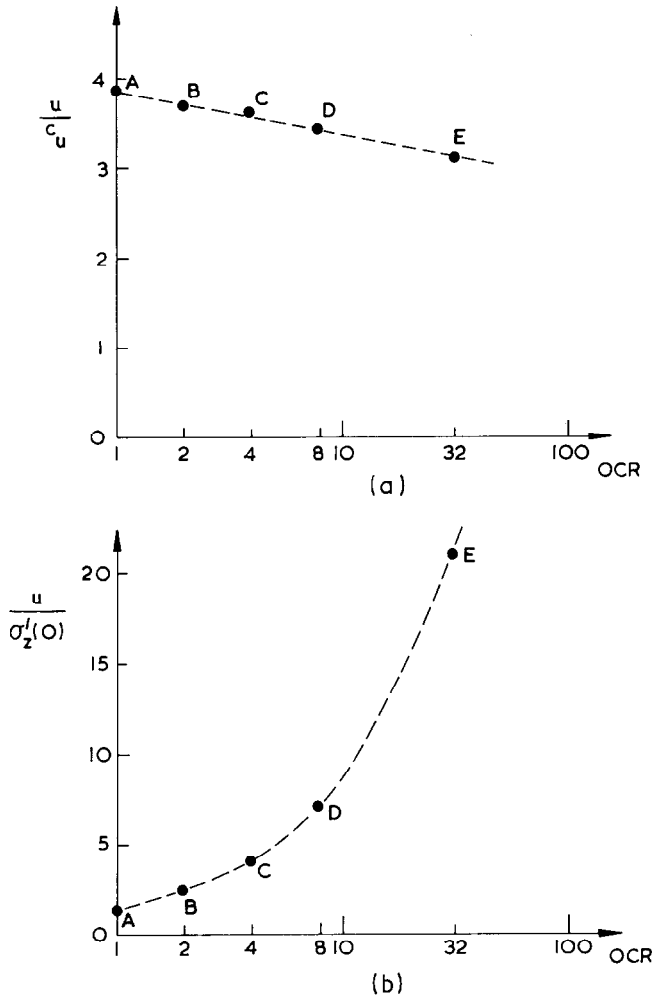

Fig. 5. Excess pore pressure near the pile face (at $r = 1{\cdot}15\ r_0$) as a function of OCR

radiating from the pile axis may occur. These cracks will be self-healing close to the pile where the soil is severely remoulded under positive effective stresses. The main effect of the presence of cracks further from the pile will be to hasten the dissipation of the excess pore pressures due to the resulting increase in radial permeability.

Stress paths for elements of soil adjacent to the pile are plotted in Fig. 8 for the soil samples A to E. Projections onto the π plane in principal stress space and also the q–p paths are shown, with effective stress paths plotted as broken curves and total stress paths as continuous curves. The stress state at the end of the expansion phase is given by points X (effective stress state) and Z (total stress state). The paths XW and ZW correspond to the stress changes during the consolidation phase (discussed later). Since each soil has the same undrained strength, all of the effective stress paths reached the critical state when $q = \sqrt{3}\ c_u$ and $p' = q/M$, i.e. point of X of Fig. 8. After failure, the increasde in total stress is borne entirely by increase in the excess pore pressure, which is indicated by section XZ and YZ of the total stress path (Fig. 8(b)).

Table 2. Comparison of stress changes due to cavity expansion in the soil immediately adjacent to the pile

Case	OCR	G/c_u	*secant* G c_u	$\Delta p/c_u$ (computer)	$\Delta p/c_u$ (eq. 9)	u/c_u (computer)	u/c_u (eq. 11)
A	1	74	30	3·62	3.40	4·20	4·02
B	2	83	83	4·14	4·42	3·96	4.23
C	4	91	91	4·50	4·51	3·90	3·91
D	8	100	100	4·64	4·61	3·72	3·72
E	32	118	118	4.66	4.77	3·42	3·59

SIMPLIFIED METHOD OF ESTIMATING STRESS CHANGES IN TERMS OF BASIC SOIL PARAMETERS

It is essential to be able to predict the stress changes around a driven pile, from basic soil parameters such as undrained shear strength and shear stiffness. The results of the parametric study for an elasto-plastic soil model may be used to form general rules for estimating the stress changes, from minimal information on the in situ soil properties. Ladanyi (1963) has pointed out that the limiting pressure needed to expand a cylindrical cavity in a real soil may be calculated from the solution for an elastic perfectly plastic material, provided a reasonable secant modulus is used for G. He suggests a secant modulus, taken from typical stress–strain curves, over the stress range zero up to half the ultimate shear stress.

A summary of the stress changes due to cavity expansion that occur immediately adjacent to the pile ($r = r_0$) is given in Table 2. It may be seen that the increase in mean total stress during cavity expansion is closely given by

$$\Delta p = c_u \ln(G/c_u) \qquad (9)$$

for values of OCR greater than 1, where the shear stress–strain curve is linear until close to failure. For OCR = 1, yield occurs immediately and the appropriate shear modulus will be less than the elastic value given in Table 1. The point to notice is that the total stress path is similar to that for the ideal elastic, perfectly plastic soil model. This result is largely due to the geometric constraints on the strain path of each soil element, i.e. they are all at different stages on the same stress–strain path (see Palmer, 1972).

Although the total stress path is largely independent of the soil model, the effective stress path (and hence pore pressures generated) will be different. For the work hardening soil model, the value of the mean effective stress changes during shearing. Thus the expression for the pore pressure generated in the region of the soil which reaches failure is

$$u = (p_i' - p_f') + 2c_u \ln(R/r), \quad r_0 \leqslant r \leqslant R \qquad (10)$$

where $(R/r_0)^2 = G/c_u$ and p_i' and p_f' are the initial and final mean effective stresses and G is the appropriate secant modulus. This situation is pictured schematically in Fig. 9.

It is important to study the effect of varying the overconsolidation ratio on the maximum value of excess pore pressure given by

$$u_{max} = (p_i' - p_f) + c_u \ln(G/c_u) \qquad (11)$$

As the value of OCR increases, so does G/c_u (keeping c_u constant as discussed above) but the value of $p_i'-p_f'$ reduces, becoming negative for values of OCR > 2 (i.e. the soil tends to dilate on shearing). These two effects virtually cancel each other out with the result that the excess pore pressure distribution for a soil of a given shear strength is almost unaffected by the past history of the soil (see Table 2). It should be noted that, as for the perfectly plastic soil

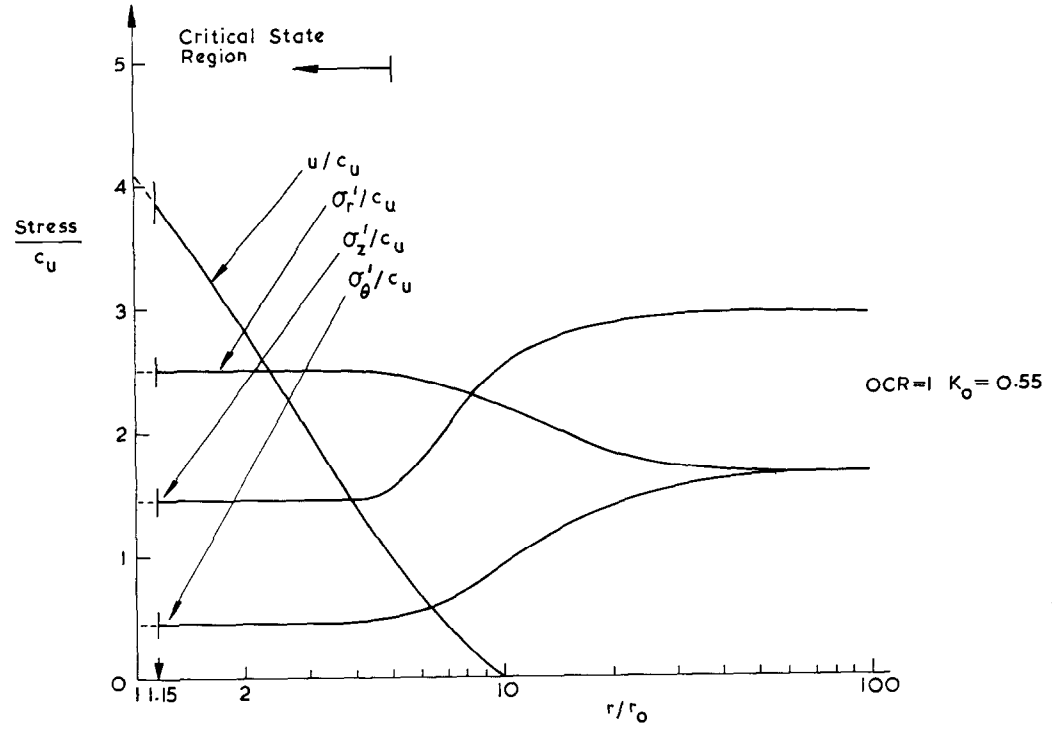

Fig. 6. Stress distributions in the soil around the pile immediately after driving, OCR = 1

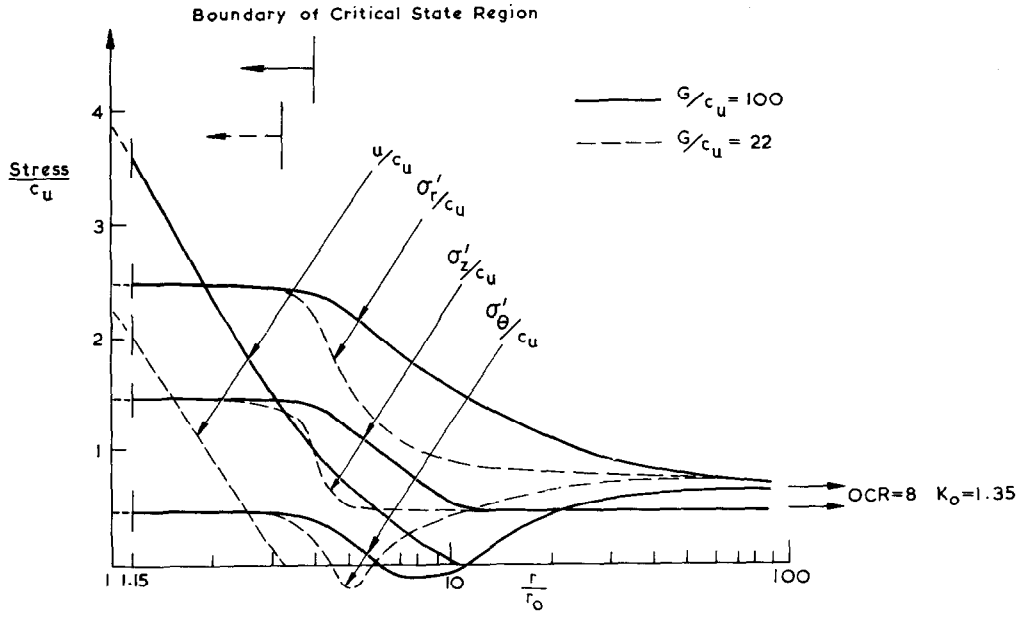

Fig. 7. Stress distributions in the soil around the pile immediately after driving, OCR = 8

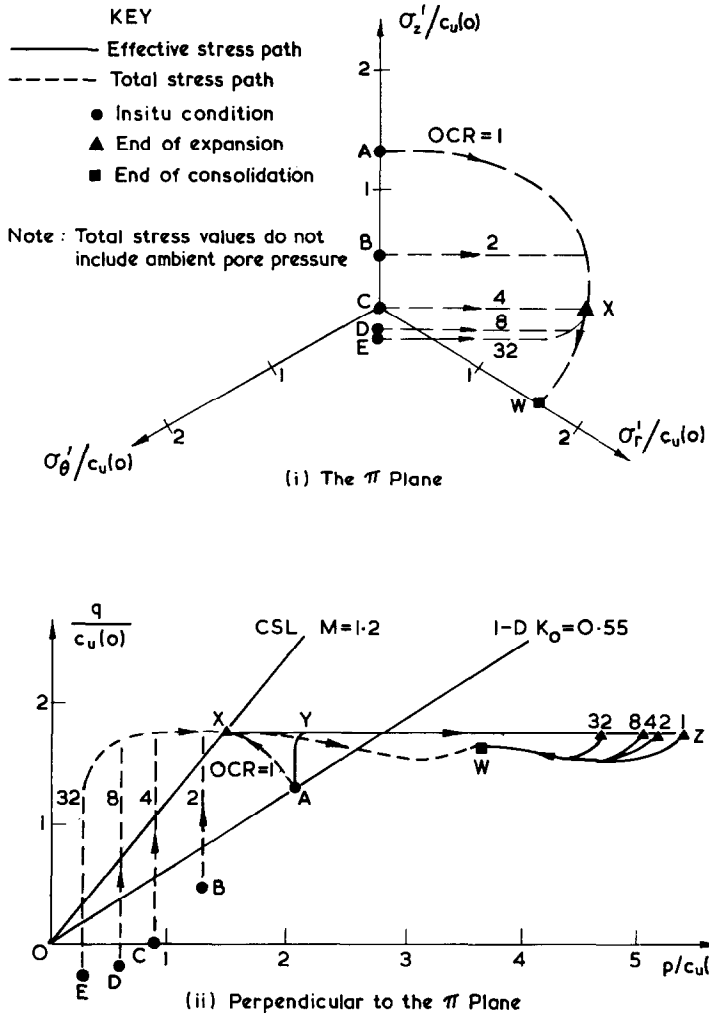

Fig. 8. Stress paths during cavity expansion and subsequent consolidation for soil at $r = 1{\cdot}15r_0$

model, the value of excess pore pressure generated decreases linearly with the logarithm of the radius at a rate of $2c_u$—see Figs 6 and 7. Figure 10 compares predictions of excess pore pressure distribution given by equation (10) with those obtained from the finite element analysis for case A. The general agreement is very good for this value of OCR, and for others. In practice, equation (10) is straightforward to apply since values of c_u and $(p_i'-p_f')$ may be obtained from standard undrained triaxial tests on undisturbed samples of soil, or alternatively, from in situ tests such as pressuremeter tests where the pore pressure is also measured. Values of the shear modulus G are best obtained from in situ tests (plate loading or pressuremeter) although high quality triaxial tests—particularly with K_0 consolidation—may also yield reasonable values for G. It will be shown later that the final stress changes around the pile are relatively insensitive to the actual choice of shear modulus.

The relative insensitivity to OCR of the excess pore pressures is partly due to the choice of variation of shear modulus G with OCR. As pointed out earlier, if the shear modulus is tied

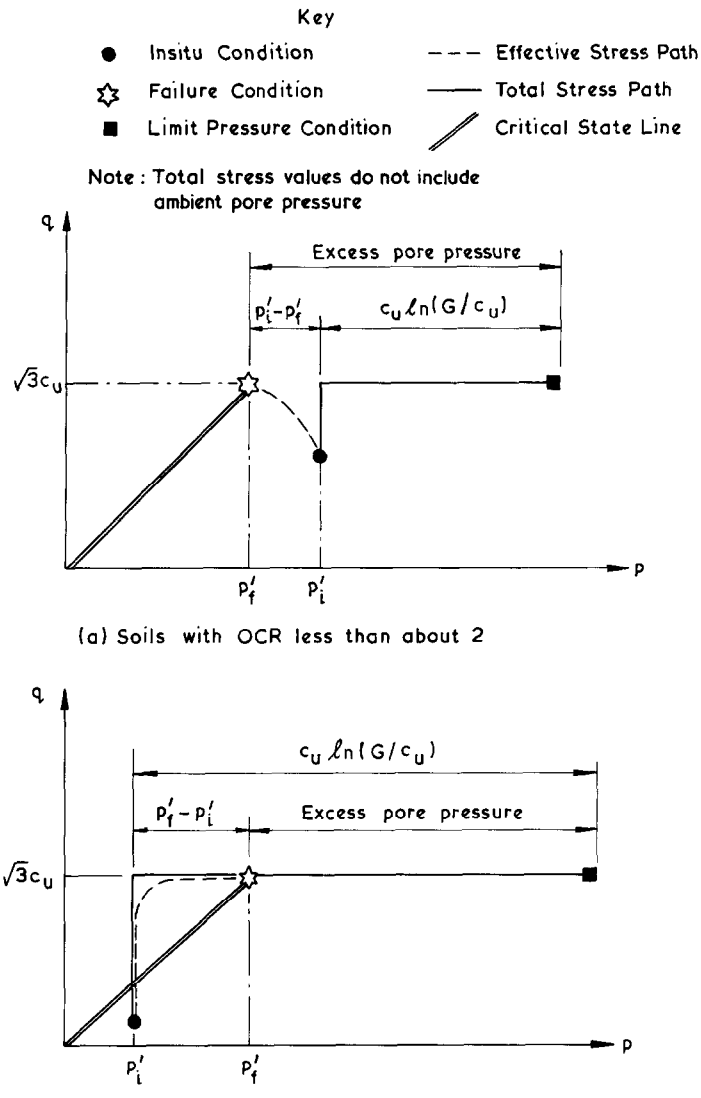

Fig. 9. Approximate stress paths during pile driving for elements of soil near to the pile

to the current effective stress level (rather than to the past maximum stress level), then lower pore pressures are generated. As would be anticipated from equation (11), the difference in pore pressure (and total radial stress) generated for the two different values of G in Fig. 7 is given by

$$u_D - u_F = c_u \ln(G_D/G_F) = c_u \ln(4{\cdot}55) = 1{\cdot}5c_u \quad . \quad . \quad . \quad . \quad . \quad (12)$$

The difference in the pore pressures for the two cases, while appreciable, does not necessarily mean that the ultimate shaft capacity of the pile is very sensitive to the choice of a value for G in the theoretical soil model. As will be shown later, when the pore pressures have dissipated, the difference in the values of the final mean effective stress for the cases D and F is about 12%.

Immediately after driving, the soil adjacent to the pile is at failure, with the effective stresses given by the conditions at the critical state in the Cam-clay model. The three principal stresses are

$$\sigma_r' = [(\sqrt{3}/M)+1]c_u \quad . . . . . (13)$$

$$\sigma_z' = p' = (\sqrt{3}/M)c_u \quad . . . . . (14)$$

$$\sigma_\theta' = [(\sqrt{3}/M)-1]c_u \quad . . . . . (15)$$

These stresses are dependent only on the values of M and c_u and not on the overconsolidation ratio. The parameter M is a function of ϕ', the angle of internal friction measured in triaxial compression, i.e.

$$M = \frac{6 \sin \phi'}{3 - \sin \phi'} \quad . . . . . (16)$$

Full knowledge of the stress state in the soil adjacent to the pile is thus readily obtainable in terms of basic engineering properties by means of equations (11) and (13) to (15).

CONSOLIDATION FOLLOWING PILE INSTALLATION

The assumptions governing the consolidation after driving, as the excess pore pressures dissipate, have been discussed by Randolph and Wroth (1979) and by Carter *et al.* (1979). Field measurements of excess pore pressures around driven piles (Cummings, Kerhoff and Peck, 1950; Bjerrum and Johannessen, 1961; Lo and Stermac, 1965; Koizumi and Ito, 1967) show that the major pore pressure gradients are radial over most of the length of the pile. Thus it will be assumed that consolidation takes place primarily by radial flow of pore water and radial movement of the soil particles. The pile will be treated as essentially rigid and impermeable.

Randolph (1977) and Randolph and Wroth (1979) have presented a solution for the radial consolidation problem, assuming that the soil deforms elastically. Under these conditions, the governing equations reduce to the same form as Terzaghi's one-dimensional consolidation equation (Terzaghi, 1943)

$$\frac{\partial u}{\partial t} = c_v \left\{ \frac{1}{r} \frac{\partial}{\partial r} \left[r \frac{\partial u}{\partial r} \right] \right\} = c_v \nabla^2 u \quad . . . . . (17)$$

where ∇^2 is the Laplace operator in polar coordinates with no variation in the θ and z direction, and c_v is the coefficient of consolidation for radial horizontal drainage. For an elastic soil, c_v will be constant and may be related directly to the permeability of the soil and the elastic properties of the skeleton by the expression

$$c_v = \frac{k}{\gamma_w m_v} = \frac{k}{\gamma_w} \frac{2G(1-\nu')}{1-2\nu'} \quad . . . . . (18)$$

where m_v is the coefficient of volume compressibility of the soil, G is the elastic shear modulus and ν' is Poisson's ratio (expressed in terms of effective stresses).

The rate of consolidation is affected by the coefficient of consolidation and the radius of the pile, r_0, and also by the size of the maximum pore pressure which, from equation (8), may be characterized by c_u and the ratio G/c_u. A suitable non-dimensional time variable for soil with a constant coefficient of consolidation has been found to be (Soderberg, 1962)

$$T = c_v t / r_0^2 \quad . . . . . (19)$$

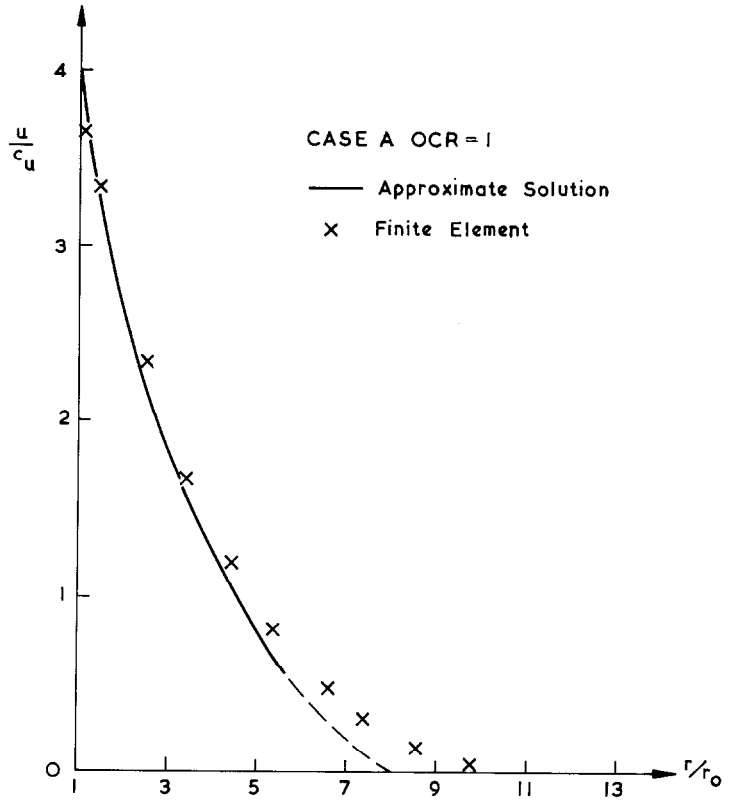

Fig. 10. Comparison of pore pressures calculated by finite element method and approximate expression—OCR = 1

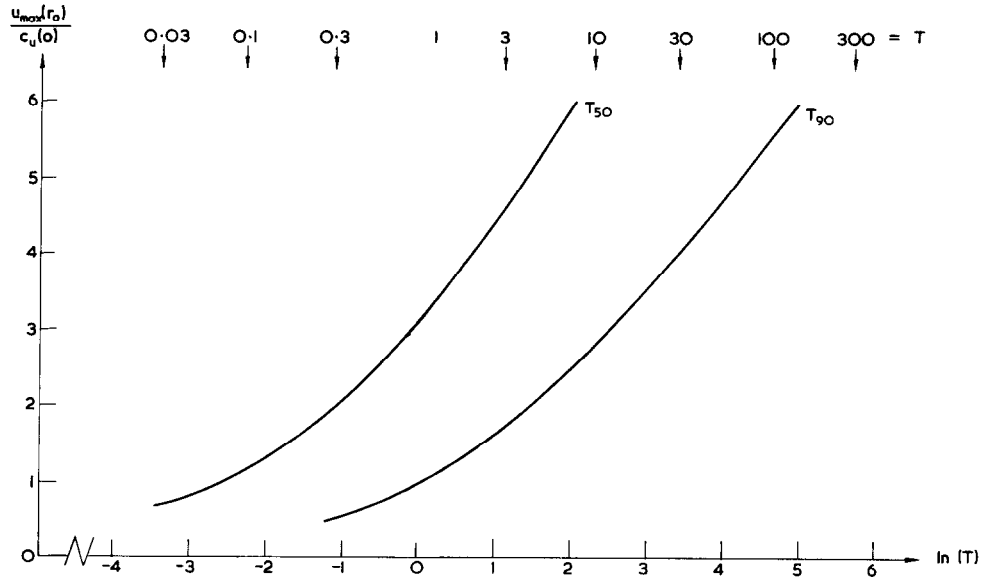

Fig. 11. Variation of times for 50 and 90% consolidation with the ratio $u_{max}(r_0)/c_u$

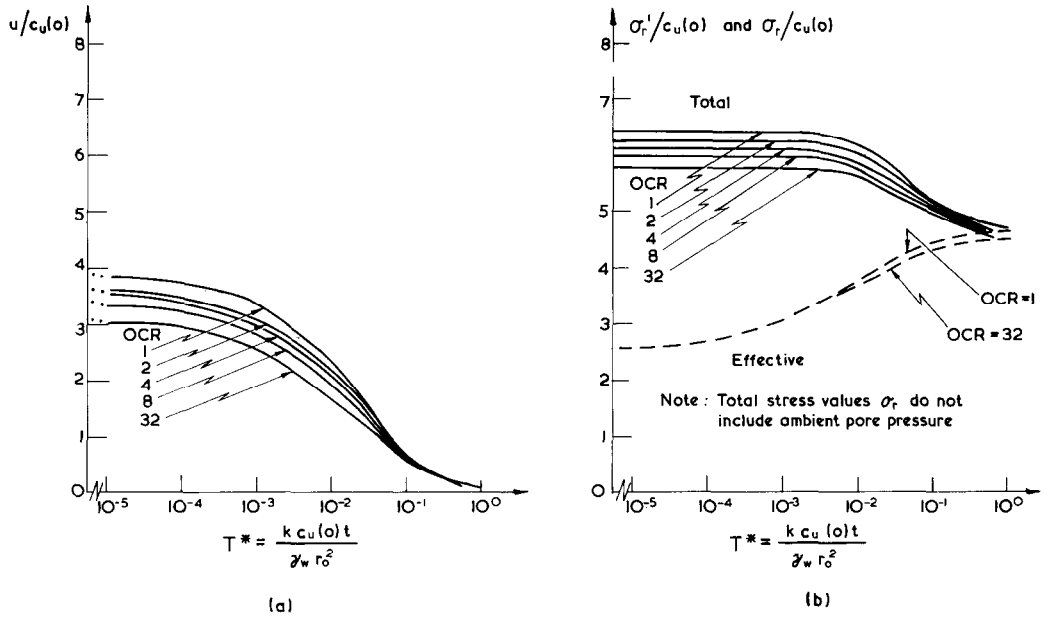

Fig. 12. Variation with time of pore pressure and radial stress at $r = 1{\cdot}15\,r_0$: (a) pore pressure; (b) effective and total radial stresses

From the analytical solutions given by Randolph and Wroth (1979) it is possible to calculate the times necessary for various degrees of consolidation to take place. Figure 11 shows a plot of the times for 50% (T_{50}) and 90% (T_{90}) consolidation to occur for different values of u_{max}/c_u. Some idea of the actual times may be obtained by considering a solid pile of radius 0·2 m driven into clay with a coefficient of consolidation of 3 m^2/year. Times for 50% and 90% consolidation would typically be of the order of 1 week and 20 weeks respectively.

The soil at radii greater than about twice the pile radius is unloading in shear during consolidation and so the solution based on an elastic soil furnishes realistic estimates of the times necessary for consolidation to take place (see Carter *et al.*, 1979). However, because the pile is relatively rigid and prevents inward movement of the soil, the soil close to the pile (where $r_0 \leqslant r \leqslant \sim 2r_0$) undergoes further increase in shear strain. A real soil will continue to yield in this region and thus it is unwise to use the elastic solution to predict the stress changes close to the pile. Since these stress changes are of utmost importance to the designer, it is necessary to go to a more realistic soil model in order to estimate them with reasonable confidence.

The finite element method has been used to investigate the stress changes during consolidation with the soil modelled as modified Cam-clay. Results are presented for the same soil parameters and (undisturbed) stress history as for the earlier analyses of undrained cavity expansion. The starting conditions for the consolidation analysis correspond to those immediately after cavity expansion (e.g. Figs 6 and 7).

The variations with time of the excess pore pressure u, the total radial stress σ_r and the effective radial stress σ_r' in the soil close to the pile are shown in Fig. 12 for all of the cases A to E. It should be noted that the coefficient of consolidation is not constant for the Cam-clay soil model. The permeability k has been taken as constant; however, the compressibility of the soil will depend on the current stress–strain response of the soil skeleton. It is possible

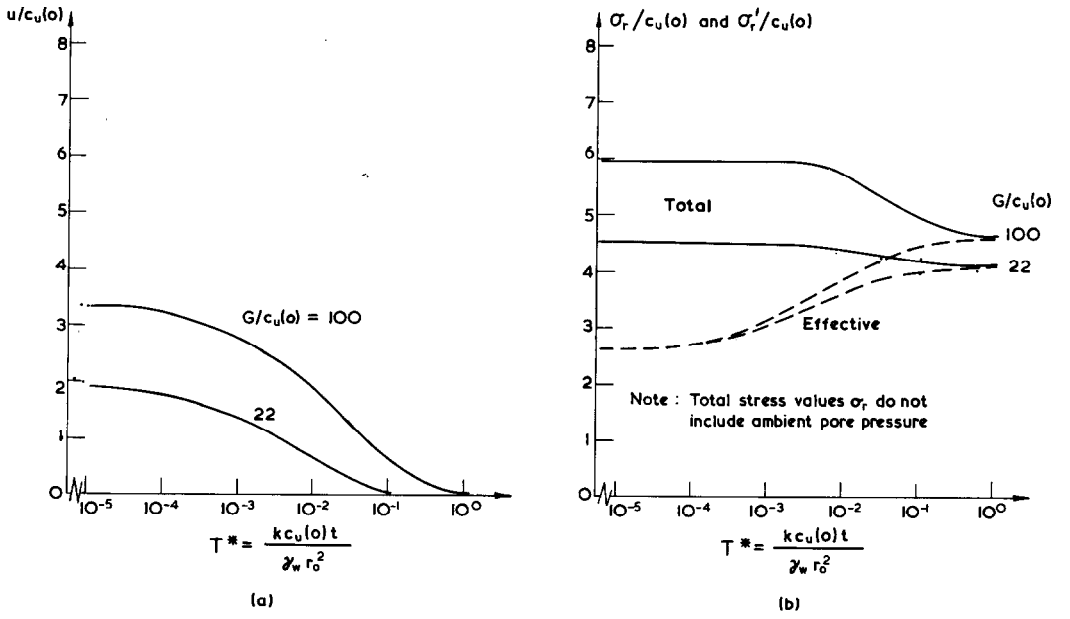

Fig. 13. Variation with time of pore pressure and radial stress at $r = 1{\cdot}15r_0$ for OCR = 8 and two different choices of elastic shear modulus: (a) pore pressure; (b) effective and total radial stresses

to relate the compressibility of the soil to the gradient of the virgin compression line (if the soil is yielding) or to the gradient of the swelling line in e–ln p' space. Thus

$$m_v = \frac{\lambda}{(1+e)\sigma_v'} \quad \text{or} \quad \frac{\kappa}{(1+e)\sigma_v'} \qquad \ldots\ldots\ldots \quad (20)$$

During consolidation around a driven pile, the soil closest to the pile will continue to yield (and thus work harden) while the soil at distances greater than about 2 or 3 pile radii from the pile axis will be unloading in shear and thus the second expression in equation (20) will be relevant for calculating m_v. The major principal stress will be σ_r' in place of σ_v'. The finite element solution takes these factors into account as well as continuously adjusting the soil compressibility according to the current value of mean effective stress p' or voids ratio e. However, this implies that there is no single value of the coefficient of consolidation c_v to insert in equation (19) to form a suitable non-dimensional time variable. For this reason, the time scale in Fig. 12 has been non-dimensionalized as T^* where

$$T^* = \frac{kc_u(0)t}{\gamma_w {r_0}^2} \qquad \ldots\ldots\ldots\ldots \quad (21)$$

The initial value of the undrained shear strength of the soil, $c_u(0)$, has been used in place of the soil stiffness $1/m_v$. The relation between T in equation (19) and T^* may be found by considering the average ratio of $1/m_v$ to $c_u(0)$. As stated previously, most of the soil will be consolidating inside the current yield locus and so the value of m_v will depend on κ in equation (20) rather than λ. Thus

$$\frac{1/m_v}{c_u(0)} = \frac{1+e}{\kappa c_u(0)}\sigma_r' \qquad \ldots\ldots\ldots\ldots \quad (22)$$

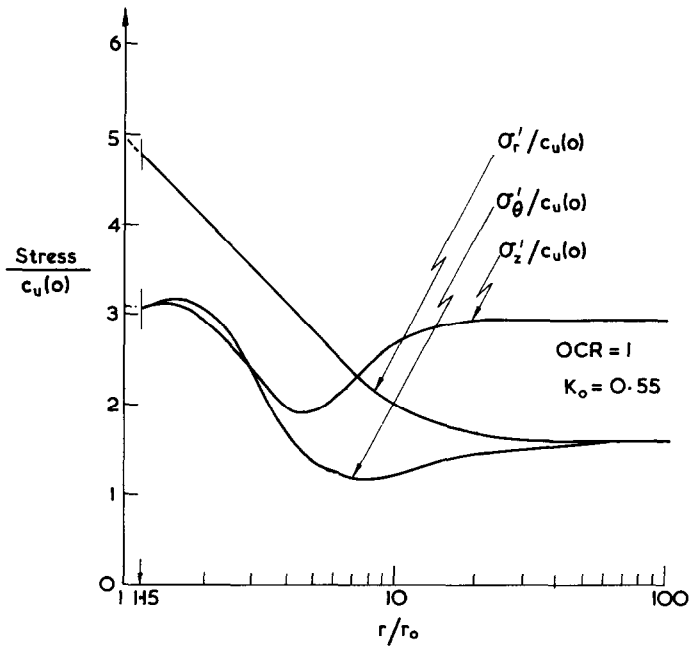

Fig. 14. Distribution of stresses at end of consolidation for OCR = 1

The average value of this ratio for the soil in question is between 200 and 250 ($\kappa = 0{\cdot}03$, $e \sim 1{\cdot}2 \rightarrow 1{\cdot}0$, $\sigma_r'/c_u(0) \sim 3 \rightarrow 4$). The variation of pore pressure given by the curves in Fig. 13(a) is similar in form to that for the elastic and elastic perfectly plastic soil models (Carter *et al.*, 1979) apart from the shift in the time scale corresponding to $T/T^* \approx 225$.

It appears from Fig. 12 that the value of OCR has only a small effect on the time for consolidation; this conclusion is, to some extent, the result of the manner in which a value for the elastic shear modulus G has been chosen for different values of OCR. Thus, if G is chosen so that it depends on the initial value of the mean effective stress (rather than on the previous past maximum stress) then less pore pressure is generated at large values of OCR during expansion. The extent to which significant excess pore pressures are generated is also reduced and consequently the time for consolidation will be reduced. To illustrate this point, Fig. 13 shows the time dependence of u, σ_r and σ_r' for cases D and F of Table 1. Except for the values of G, which differ by a ratio of 4·5, the soil properties are identical with OCR = 8. As expected, for the soil with the larger value of G, excess pore pressures are generated over a wider zone during cavity expansion and take longer to dissipate. After consolidation, the radial effective stress acting on the pile is greater for the soil which is elastically stiffer. However, it should be noted that, although the ratio of the elastic shear moduli is 4·5 and the ratio of the pore pressures generated during cavity expansion is 1·8, the ratio of the final radial effective stresses acting on the pile is only 1·13 (see Fig. 13(b)). Similarly, the final undrained shear strengths of the soil close to the pile (which may be calculated from the final effective stress state) differ by only 12% (see Fig. 18).

Distributions of stress in the soil once consolidation is complete are plotted in Figs 14 and 15 for the two soils with OCR = 1 and 8 respectively (cases A and D of Table 1). Pile driving has significantly altered the stresses in the soil out to about 20 pile radii. The radial effective stress acting on the pile has a value of about five times the in situ strength, $c_u(0)$, this result

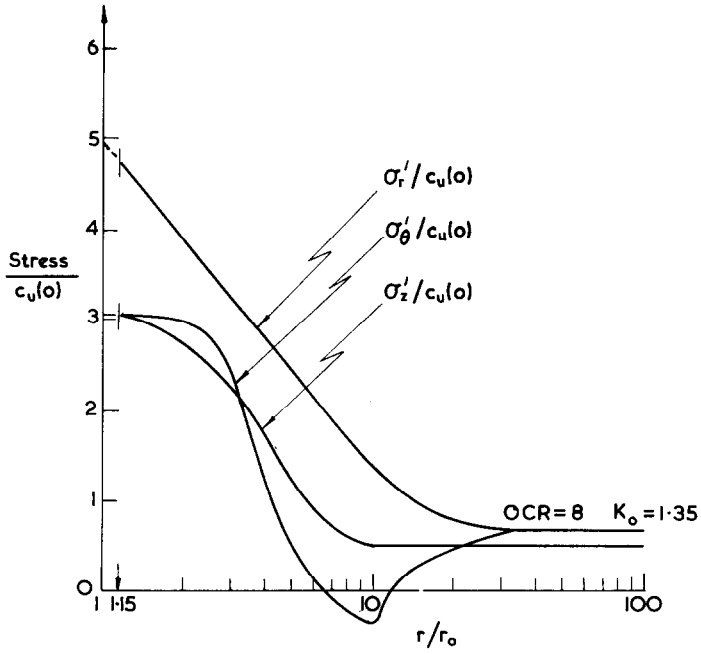

Fig. 15. Distribution of stresses at end of consolidation for OCR = 8

being true for all OCR in the range 1 to 32. The decay of σ_r' is approximately logarithmic with radius until it reaches the in situ value at about $20r_0$.

Some idea of the stress paths followed by elements of soil close to the pile can be gained from Fig. 8. All of the cases A to E inclusive are shown, with effective stress paths plotted as broken lines and total stress paths plotted as continuous lines. Ambient pore water pressures have not been included in the plots of total stress. Thus, starting from points X and Z (the stress states at the end of expansion), the effective and total stress paths converge until they meet at point W at the end of consolidation. All soil samples end expansion and begin consolidation with the same effective stress state on the p–q and the π plane plot; this is because all cases were specially chosen to have the same initial value of undrained strength $c_u(0)$. On both the π plane projection and the p–q plot the stress paths during consolidation are almost the same; they are practically independent of the initial value of OCR for the soil. Close to the pile the soil has 'forgotten' its in situ condition before pile driving. After consolidation all soil samples are left in a stress condition with equal minor principal stresses where the radial effective stress component is the major principal stress, having a value of about five times the original undrained strength. The ratio of $\sigma_z' = \sigma_\theta'$ to σ_r' after consolidation is about 0·65.

The variation with time of the undrained strength c_u of the soil adjacent to the pile is plotted in Fig. 16. After pile driving the undrained strength increases significantly with the passage of time. Throughout the range of OCR from 1 to 32 the ultimate strength of the soil $c_u(\infty)$ is nearly the same; this is about 60% greater than the initial in situ value $c_u(0)$. The radial distributions of $c_u(\infty)$ have been plotted in Fig. 17. Again in each case this ultimate strength decreases with the logarithm of the radius until it reaches the in situ value $c_u(0)$ at about 10 pile radii.

Since the final strength of the soil decreases with distance from the pile, it is necessary to check that failure will still develop on the pile–soil interface when the pile is loaded and not

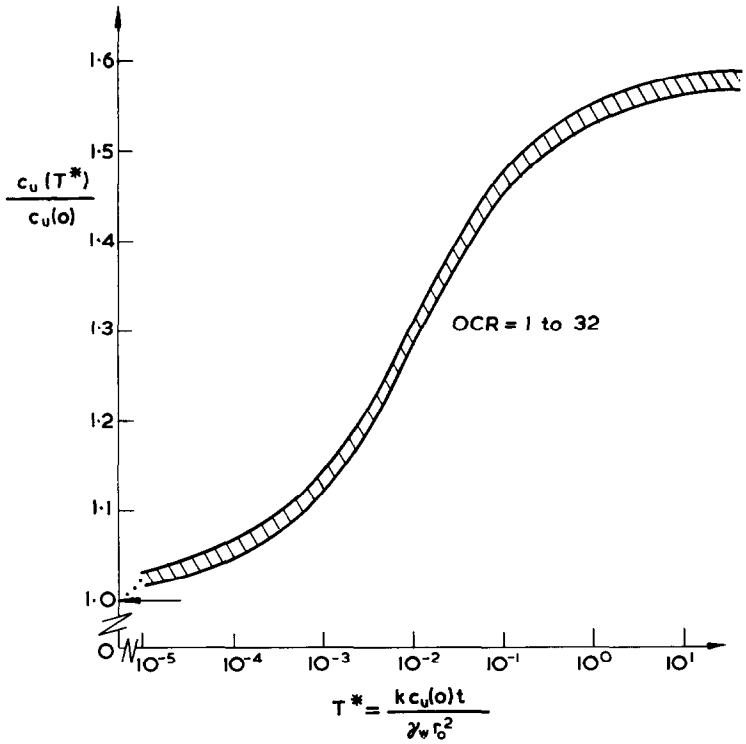

Fig. 16. Variation with time of undrained shear strength of soil at $r = 1{\cdot}15\, r_0$

within the soil at some distance from the pile. The shear stress distribution in the soil around a vertically loaded pile may be deduced by considering vertical equilibrium (Cooke, 1974). The shear stress decreases in inverse proportion to the radius from the pile centre-line. This decrease with radius is much more rapid than that of the new undrained shear strength, $c_u(\infty)$; this is shown by the dashed line in Fig. 17 where, for the sake of argument, it has been assumed that a shear stress of $c_u(\infty)$ has been developed at the pile shaft, i.e. at $r = r_0$. It may be seen that the ratio of the available shear strength to the induced shear stress is still lowest at the pile–soil interface in spite of the decrease in strength with radius. Although the distribution of strength with radius will vary depending on the degree of consolidation (i.e. on the time since installation of the pile) the rapid decrease with radius of the shear stress induced by loading the pile implies that failure will always occur on the pile–soil interface.

EFFECT OF CONSOLIDATION ON PILE DESIGN

There has been much discussion over the past few years on the relative merits of effective stress and total stress methods of predicting shaft capacity of a pile (Tomlinson, 1971; Burland, 1973; Parry and Swain, 1977a and 1977b). The total stress approach seeks to relate the adhesion on the pile–soil interface to the original in situ shear strength of the soil by means of an empirical α factor. This factor lumps together all the effects of disturbance caused by installation of the pile and, as such, may vary considerably depending on the type and method of installation of the pile, the sensitivity of the soil and the past stress history of the soil. On the other hand, the effective stress approach as presently used (Burland, 1973; Parry and

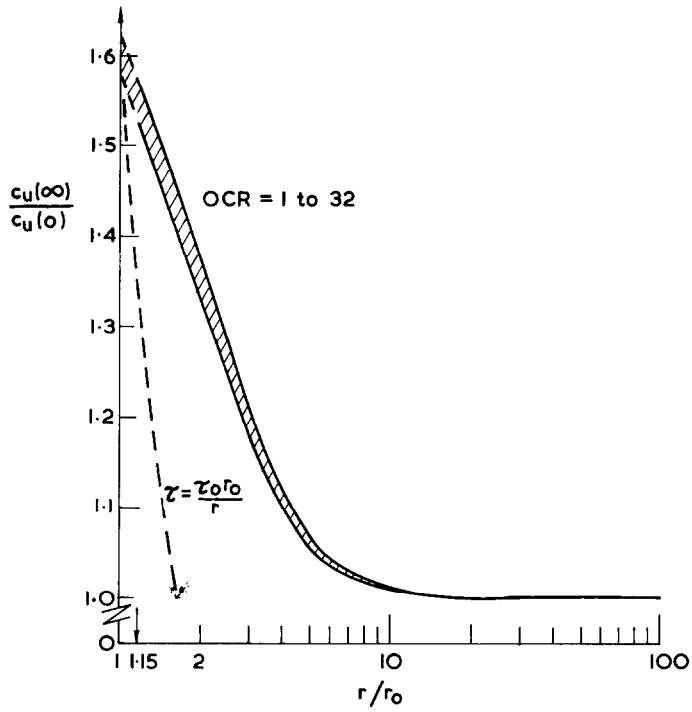

Fig. 17. Distribution of soil strength with radius and comparison with possible shear stress distribution

Swain, 1977a and 1977b) leads to estimates of the limiting friction on the pile shaft in terms of the assumed effective stresses acting around the pile. Until recently (Kirby and Wroth, 1977; Esrig *et al.*, 1977; Esrig and Kirby, 1978) little attempt has been made to estimate the effective stresses acting round the pile by considering the nature of the disturbance caused by installation of the pile.

The ideas presented in this Paper enable two important contributions to be made to the above methods. Firstly, the effective stress state around the pile may be estimated at the end of consolidation. An effective stress method of design of pile shaft capacity may thus be formulated in terms of this stress state and the changes in effective stresses which will occur when the pile is loaded. The second contribution, which may be seen as an indirect form of effective stress design, is that the Cam-clay soil model enables a new intrinsic undrained shear strength to be calculated for the soil close to the pile at the end of consolidation.

From Fig. 5, the excess pore pressure generated during pile installation at the pile face varies from nearly 4 times the original undrained shear strength for OCR = 1, down to about $3{\cdot}3c_u$ at high OCR. The increase in radial effective stress during the consolidation phase (see Fig. 12) varies from 54% of the initial excess pore pressure (OCR = 1) up to nearly 60% (OCR = 32). Combining these two sets of results, the increase in the radial effective stress during consolidation is of the order of twice the original undrained shear strength regardless of the initial value of the overconsolidation ratio. Using equation (13), the final radial effective stress after consolidation will be of the order of $(\sqrt{3}/M+3)c_u$. Assuming that the state of the soil close to the pile ends up on the one dimensional virgin consolidation line, the new voids ratio and associated strength of the clay may be calculated. For Boston blue clay, $M = 1{\cdot}2$ and the ratio (c_u/σ_c') for one dimensional consolidation is given by the Cam-clay model as 0·34.

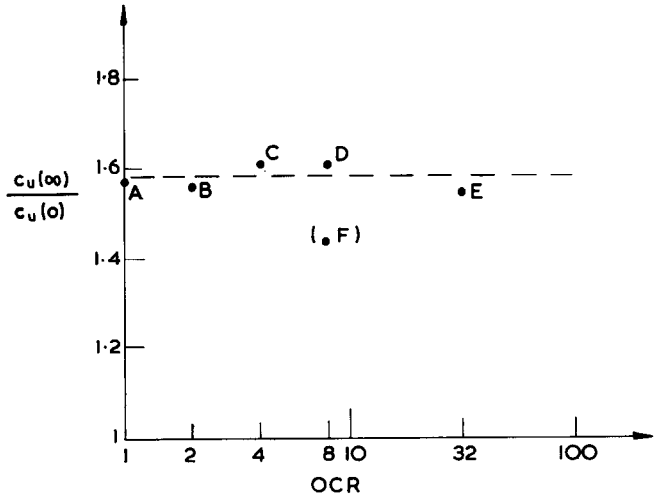

Fig. 18. Variation of ratio of final to initial undrained shear strength with OCR

Thus the final undrained shear strength close to the pile may be estimated as

$$c_u(\infty) = 0{\cdot}34 \times (\sqrt{3}/1{\cdot}2 + 3)c_u(0) = 1{\cdot}51\ c_u(0)$$

The actual computed values of $c_u(\infty)/c_u(0)$ are plotted against OCR in Fig. 18. Apart from small variations, the ratio is approximately constant (for the chosen soil parameters) at about 1·6, which agrees well with the approximate ratio estimated above.

It is necessary at this stage to emphasize again the assumptions made in the analysis, particularly those regarding plane strain conditions and the ignoring of shear stresses in r–z planes. Shear stresses will be present not only due to residual driving stresses but also to balance the high total vertical stresses which occur during pile driving. Field measurements have shown that excess pore pressure greater than the existing effective overburden stresses are generated during pile installation. The resulting changes of total vertical stress must be balanced by shear stresses in the soil around the pile in order to maintain vertical equilibrium. The effect of the presence of these shear stresses, and any resulting out of plane (vertical) soil movement, on the conclusions above must be investigated at a later date, perhaps by means of a full two-dimensional (axisymmetric) finite element analysis.

EFFECT OF SOIL SENSITIVITY

One of the features of soil behaviour which has been ignored in the analysis so far is the reduction in soil strength as it is remoulded, i.e. the sensitivity of the soil. Immediately after driving, the strength of the soil close to the pile will be the remoulded strength not the peak strength. The ratio of peak strength to remoulded strength of the soil may vary from unity (or just below for stiff fissured clay) to between five and ten for a typical sensitive clay. The sensitivity tends to be higher for normal or lightly overconsolidated clay than for heavily overconsolidated clay. Skempton and Northey (1953) discuss some of the reasons for sensitivity in clay. Clearly if an attempt is to be made to predict the final soil strength around a driven pile, then the sensitivity of the soil must be taken into account. This necessitates attempting to model the phenomenon of soil sensitivity in terms of critical state soil mechanics and the Cam-clay model.

Critical state soil mechanics is based on the concept that there exists a unique line of critical

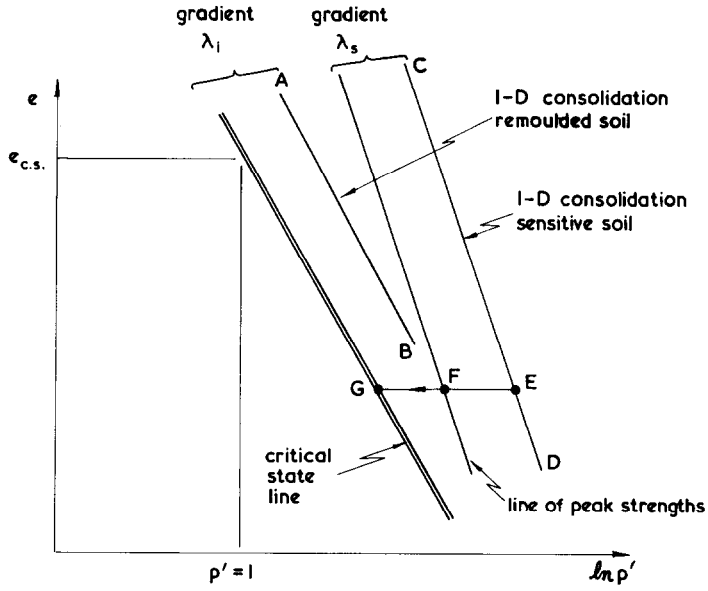

Fig. 19. Lines of one dimensional consolidation, peak strengths and critical states for a sensitive soil

states in q–p'–e space at which a particular soil will flow without further change in effective stresses or voids ratio, e. A projection of this line onto the e–ln p' plane gives a straight line which is parallel to the virgin consolidation line and whose position may be defined by the value of e_{cs}—defined as the voids ratio at the critical state for unit mean effective stress (see Fig. 19). During one dimensional consolidation, a sensitive clay will reach equilibrium at a higher voids ratio for a given mean effective stress than an insensitive clay. Referring to Fig. 19, while the consolidation path for an insensitive clay would be as shown by the straight line AB of gradient λ_i, the path for a sensitive clay as deposited naturally, might be shown by the straight line CD of gradient λ_s. If a sensitive soil is normally consolidated at E and is then sheared with no drainage allowed, it will exhibit a peak shear strength (at some point F) before its structure (which is at an artificially high voids ratio) collapses. The final remoulded strength of the soil is given by its position G on the critical state line. A feature of the shearing of a sensitive clay is that high pore pressures are generated as the soil is remoulded and the effective stress drops from point E to point G in Fig. 19.

A suggested model of this behaviour is depicted in Fig. 20, which shows projections of the effective stress path on the q–p' plane and on the e–p' plane. In addition to the line of critical states, a line of peak shear strengths has been postulated. Limited experimental evidence (Yudhbir, 1973) suggests that this line will be parallel to the normal consolidation line of gradient λ_s on an e–ln p' plot. On the q–p' plane, however, it is believed that the peak strength and remoulded strength occur at the same critical stress ratio given by the Cam-clay parameter M. Thus, in Fig. 20, soil initially at state E will follow an effective stress path EF (for undrained shear) until a peak deviator stress of q_F is reached. As the soil continues to shear, the stress ratio q/p' remains constant but the mean effective stress decreases as the soil structure tends to collapse until the critical state is reached at G. The sensitivity of the soil is then given by $S_t = q_F/q_G$. The path from F to G is accompanied by the generation of large pore pressures. The overall total stress path will of course depend on the form of shear test, while the effective stress path is taken to be unique for an undrained test.

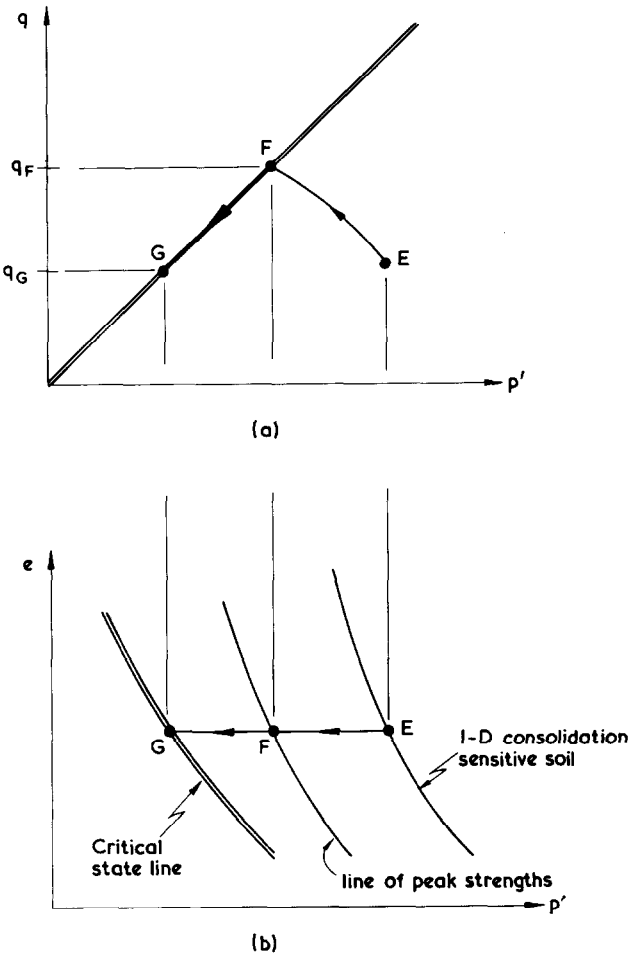

Fig. 20. Undrained stress path in q–p'–e space for sensitive soil: (a) path in q–p' space; (b) path in e–p' space soil: (a) assumed variation of shear strength of soil with radius; (b) stress–strain curve implied by (a)

The first part of the undrained path EF is given by fitting the Cam-clay model to the known initial conditions at E and adopting the critical state stress ratio given by the parameter M. In effect this makes the line of peak strengths into a quasi-critical state line for the sensitive soil, of gradient λ_s. The decrease in mean effective stress between E and F may be calculated on the assumption that the form of the stress path EF in q–p' space is the same as that for an insensitive soil. This is equivalent to assuming that the ratio of κ_s (the slope of the swelling line for sensitive soil in e–ln(p') space) to λ_s is the same as the ratio κ_i/λ_i.

The subsequent behaviour FG consists of the state of the soil moving down the line of critical stress ratio (while remaining at constant water content) until reaching the critical state line appropriate to the remoulded soil. An estimate of state G requires knowledge of e_{cs} and λ_i.

In order to apply the model postulated above to the problem of cavity expansion, some assumption must be made about the level of shear strain necessary to produce a given degree of softening (i.e. a given reduction in strength). When a cylindrical cavity is created, the radius

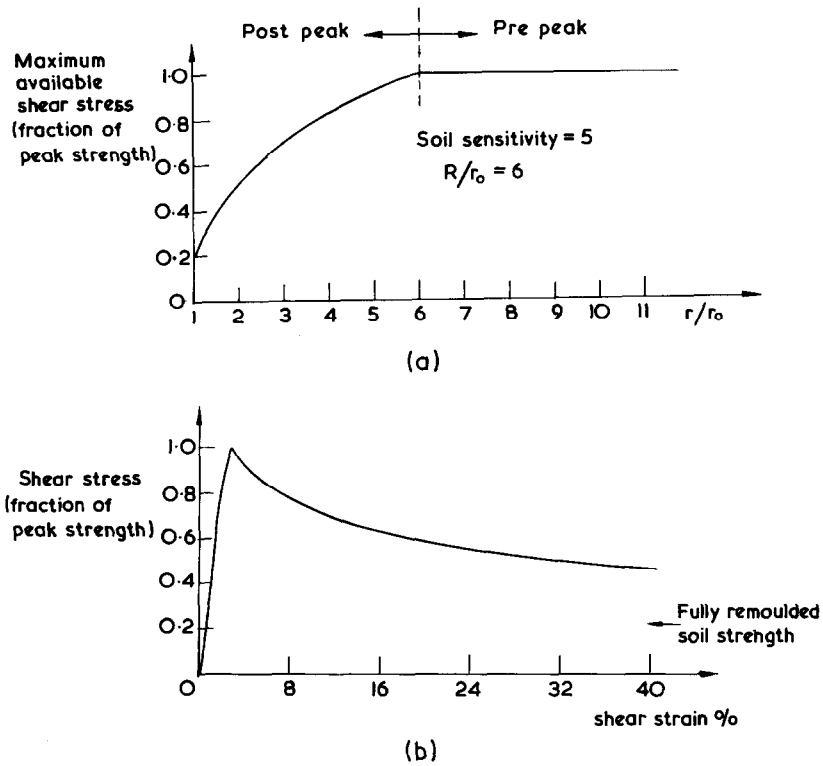

Fig. 21. Example of assumed variation of soil strength with radius and implied stress–strain curve for sensitive

at which the soil is just at its peak strength is given as before by

$$R/r_0 = \sqrt{(G_{sec}/c_u)} \quad . \quad . \quad . \quad . \quad . \quad . \quad . \quad . \quad . \quad . \quad (23)$$

where G_{sec} is the appropriate secant shear modulus, and c_u is the peak shear strength. Thus at $r = R$, the soil will be at its peak strength (equivalent to position F in Fig. 20) while at the pile–soil interface, $r = r_0$, the soil will be completely remoulded (position G in Fig. 20). Since it is believed that the region of severe remoulding is restricted to a zone close to the pile, the assumption has been made that the maximum shear stress available to the soil varies linearly with the logarithm of the radius from peak strength at $r = R$ to remoulded strength at $r = r_0$. This variation is shown in Fig. 21(a) for a typical value for R/r_0 of 6 and a sensitivity of 5.

The particular variation of soil strength between $r = r_0$ and $r = R$ has been chosen to enable the radial equilibrium equation to be integrated in order to deduce the initial pore pressure distribution. This distribution is not particularly sensitive to the exact variation of strength with radius which is chosen. The form of the shear stress–strain curve for a strain-softening soil is thus determined by the value of R/r_0 (calculated from equation (23)) and the soil sensitivity, since both shear stress and shear strain are now known functions of radius. The resulting implied stress-strain curve for soil where $R/r_0 = 6$ and $S_t = 5$ is shown in Fig. 21(b).

The effect of soil sensitivity on pore pressures generated during pile driving and on the subsequent stress changes during consolidation is best seen from the comparison with actual field tests on piles, described in the following section. As a general principle, mean total stress increases by between 3 and 4 times the peak undrained shear strength during pile driving—as

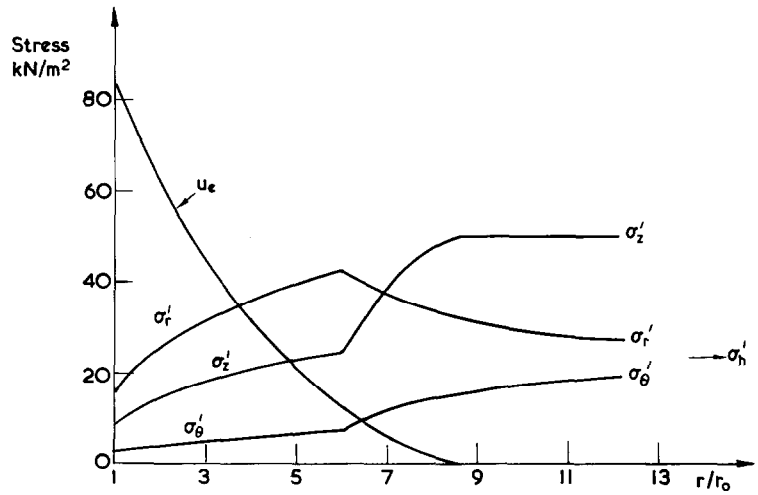

Fig. 22. Predicted stress distribution immediately after driving for the case reported by Seed and Reese (1955)

was the case for insensitive clay. However, additional pore pressures are generated due to the large drop in mean effective stress which occurs on remoulding of the clay.

COMPARISONS WITH FIELD TESTS ON PILES

It is hoped that modelling the processes of pile installation and subsequent consolidation of the soil will eventually form the basis of an effective stress method of design for piles driven into cohesive soil. Before progressing to the point where the long-term shaft capacity of a pile may be predicted, it is necessary to check that the main features of the model are borne out by results from field tests, particularly as regards the increase in strength of soil adjacent to a driven pile. To accomplish this, case records must be studied where soil samples have been taken from close to the pile at different times after driving. There is a great paucity of such good quality data; the authors have found only two cases—Seed and Reese (1955) and Eide *et al.* (1961)—where information was obtained on the changes in water content and strength of the soil adjacent to a driven pile. In addition, both cases report the results of pile load tests carried out at different time intervals in order to determine the variation of bearing capacity with time after driving.

Tests reported by Seed and Reese (1955)

Seed and Reese (1955) report the results of an investigation where several closed ended piles were driven into a layer of organic silty clay at a site near San Francisco. One of the piles, instrumented with strain gauges, was load tested to failure at intervals after driving in order to measure the change in bearing capacity with time. To assess the changes with time in soil properties close to a pile, soil samples were obtained at different times after driving, adjacent to similar piles driven in the vicinity of the main test pile.

The test pile (radius 76·2 mm) was installed through a sleeve, penetrating the silty clay from 2·75 m to 7 m depth. The soil strength profile was reasonably uniform over the length of embedment with average peak and remoulded shear strengths (measured in unconfined compression) of 12 kN/m^2 and 5·5 kN/m^2 and water content of 48·1%. The plasticity index was 18% (Liquid Limit of ~41%) from which a value of ϕ' has been estimated as 32° giving

$M = 1{\cdot}29$. Remoulded clay was consolidated to three different pressures and then tested in unconfined compression. The three resulting strengths and the strength of soil remoulded at its natural water content fell on a strain line when plotted on a logarithmic scale against water content. The gradient of this line (assuming the specific gravity of the soil particles is $G_s = 2{\cdot}7$) yields a value for λ_i of 0·19 and the position of the line gives $e_{cs} = 1{\cdot}73$. A value of κ will be taken as 0·04. At the pile mid-depth, the effective vertical stress is $\sigma_v' = 50$ kN/m^2 (ambient pore pressure is $u_0 = 35$ kN/m^2 and the saturated unit weight of the soil is $\gamma_s = 18$ kN/m^3). Assuming a value for K_0, given by $1 - \sin\phi'$, of 0·47, the horizontal effective stress at the pile mid-depth is $\sigma_h' = 23{\cdot}5$ kN/m^2 and the mean effective stress is $p' = 32{\cdot}3$ kN/m^2.

With these soil parameters and initial stresses, the model for sensitive clay described previously predicts a peak shear strength (state F in Fig. 20) of 15·5 kN/m^2. The values of λ_i and e_{cs} were deduced from the remoulded strength data, so the model necessarily gives the measured remoulded strength (state G) of 5·5 kN/m^2. Hence the sensitivity of the soil is computed to be 2·86. This figure and that for the peak strength are in reasonable agreement with the measured values.

From a finite element analysis of cavity expansion assuming an insensitive soil with an undrained shear strength of 15·5 kN/m^2, it is possible to establish the limit of the failed zone of material around the driven pile—that is the value of R/r_0. With this value and a sensitivity of 2·86, the stress distribution around the driven pile may be calculated analytically following the principles outlined previously. This distribution is shown in Fig. 22. It may be seen that the effective stress state is no longer constant within the failed zone as was the case for an insensitive soil (see Figs 6 and 7). The maximum pore pressure generated is predicted to be 84 kN/m^2 which is 4·7 times the peak plane strain strength ($= 2 \times 15{\cdot}5/\sqrt{3} = 17.9$ kN/m^2). The excess pore pressure is due to a drop in mean effective stress from 32·3 kN/m^2 down to 8·7 kN/m^2 (a drop of 1·3 times the peak shear strength) together with an increase in mean total pressure of 60·9 kN/m^2 (3·4 times the peak shear strength). During subsequent consolidation, the stresses at the pile face change until at the end of consolidation the two minor principal stresses, σ_θ' and σ_z', are equal at a fraction of 0·62 times the major principal stress, σ_r'. The mean effective stress is predicted to increase from 8·7 kN/m^2 to 43·6 kN/m^2, accompanied by an increase in the remoulded strength of the soil to a final value of 18·2 kN/m^2. The change in water content may be calculated assuming that it varies linearly with the logarithm of the soil strength with a gradient λ_i equal to that of the virgin consolidation line. This assumption gives a long term water content for the soil adjacent to the pile of 39·3%. The figures for the final strength and water content of the soil are bounds (upper and lower, respectively) on the values measured at 33 days which were a strength of 18 kN/m^2 and water content of 41·1%.

Seed and Reese (1955) quote values of the soil permeability of about 2×10^{-10} m/s at a water content of 40%. It is likely that the in situ permeability will be higher than this since the natural water content is 48·1% and laboratory estimates of permeability tend to be much too low. A value of permeability of $k = 10^{-9}$ m/s has been assumed in order to calculate the change in soil strength with time. In Table 3 a comparison is given of the values of predicted soil strength and water content with those measured by Seed and Reese at one day and 33 days after pile installation. Unfortunately the remoulded strengths of these soil samples were not measured but the new sensitivity after remoulding is unlikely to be high. The two sets of figures are in encouragingly good agreement, especially in view of the likelihood of some disturbance occurring when samples are obtained close to a driven pile.

It may be noted that it is possible to use the approximate design rules (given at the end of the section entitled 'Effect of consolidation on pile design') to estimate the final water content and strength of the soil close to the pile. Working with the measured soil properties, the

Table 3. Measured and predicted changes in soil strength and water content (data from Seed and Reese, 1955)

Time after driving	Undrained shear strength, triaxial: kN/mF			Water content: %	
0 (in situ)	peak	12	15.5	48·1	48·1
	remoulded	5·5	(5·5)		
1 day	peak	16	—	43.6	42.9
	remoulded	—	11·1		
33 days	peak	18	—	41·1	39·4
	remoulded	—	17·9		
		field	analytical	field	analytical

excess pore pressure generated during driving may be estimated as 4 times the peak plane strain shear strength ($12 \times 2/\sqrt{3} = 13{\cdot}9$ kN/m^2) with an additional amount due to the drop in mean effective stress level as the soil is remoulded. This latter amount is due to a reduction in shear strength from 12 kN/m^2 to 5·5 kN/m^2 and will entail a decrease in mean effective stress of $\Delta p' = \Delta q/M = 2(12-5{\cdot}5)/1{\cdot}29 = 10$ kN/m^2. Thus the total excess pore pressure generated will be approximately 66 kN/m^2. From the results for Boston blue clay, some 54 to 60% of the excess pore pressure is returned as an increase in radial effective stress during consolidation. Taking the lower figure of 54%, and using equation (13) for the radial effective stress immediately after driving, the final radial effective stress may be estimated as

$$\sigma_r' = [(\sqrt{3}/M)+1]c_u(0)+0{\cdot}54 \times 66 = 51 \text{ kN/m}^2 \quad . \quad . \quad . \quad . \quad (24)$$

where $c_u(0)$ is the remoulded plane strain shear strength, taken as $5{\cdot}5 \times 2/\sqrt{3} = 6{\cdot}4$ kN/m^2. The Cam-clay model indicates for this soil a $(c_u/\sigma_c')_{nc}$ of 0·31, so the final shear strength of the soil adjacent to the pile is 16 kN/m^2. The corresponding water content is obtained using the value of $\lambda = 0.19$ as 40·6%. These values are in reasonable agreement with the measured values, with the estimated soil strength being on the conservative side.

When a pile is loaded, the effective stresses around the pile will change. Also, the adhesion between pile and soil will, in general, be lower than the undrained shear strength of the soil. Seed and Reese (1955) report that after 33 days the average adhesion was only ~12 to 13 kN/m^2 compared to the measured soil strength of 18 kN/m^2. However, it is instructive to plot the computed soil strength, normalized by the long term strength, as a function of time and compare the variation with the measured capacity of the pile, normalized by the final bearing capacity. This is shown in Fig. 23. It may be seen there is reasonable agreement between the predicted increase in soil strength and the measured increase in bearing capacity.

Tests reported by Eide et al. *(1961)*

Tests on a tapered timber pile driven into sensitive, normally consolidated clay at Drammen, Norway, are reported by Eide *et al.* (1961). The soil profile shows a dry crust approximately 3·5 m thick below which is a silty marine clay whose strength increases proportionally with depth. The pile, tapering from 0·175 m radius down to 0·075 m radius, was driven from an excavated pit 2·4 m deep to a total penetration of 13·1 m (leaving the tip some 15·5 m below ground level). The plasticity index of the clay was reasonably constant at 20% and so a value of ϕ' will be assumed of 30° (giving $M = 1{\cdot}2$). From values of the compression index quoted

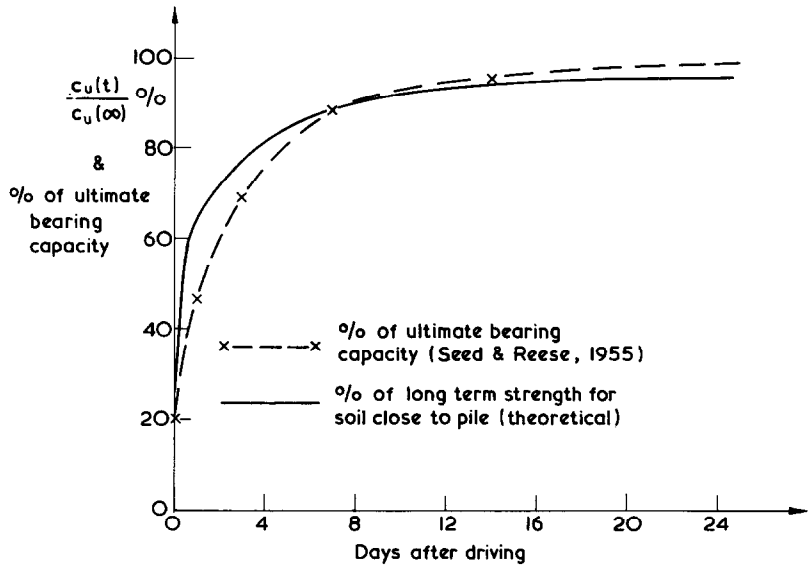

Fig. 23. Comparison of measured increase in bearing capacity of pile with theoretical increase in strength of soil close to pile (data from Seed and Reese, 1955)

by Eide *et al.*, λ_i may be estimated as 0·15 and κ_i will be taken as 0·03. The stress conditions at a depth of just under 10 m will be considered in detail as samples from close to the pile were recovered from this depth some three years after the original driving of the pile.

At 9·5 m depth, the stress conditions are $\sigma_v' = 95$ kN/m^2 (ambient pore pressure of $u_0 = 80$ kN/m^2, $\gamma_s = 18{\cdot}4$ kN/m^3) and assuming a K_0 of about 0·5, $\sigma_h' = 47{\cdot}5$ kN/m^2, giving $p' = 63{\cdot}3$ kN/m^2. The natural water content was 35% which is equivalent to a voids ratio of 0·945 (taking $G_s = 2{\cdot}7$). The strength of the soil measured by vane, cone and unconfined compression tests varied between 17 and 20 kN/m^2 at peak, falling to a remoulded value of 4 kN/m^2 ($S_t \sim 5$). The model for sensitive clay yields a peak strength of 28 kN/m^2, which is somewhat higher than the measured peak strengths. This may be due to the assumption in estimating the position of F in Fig. 20 (that $\kappa_s/\lambda_s = \kappa_i/\lambda_i$) or may merely reflect some disturbance having taken place in obtaining the field peak strengths. A value of e_{cs} of 1·23 is chosen in order to obtain the measured remoulded strength of 4 kN/m^2 at the natural water content, giving a computed sensitivity of 7.

Following the same finite element procedure as for the Seed and Reese case study, the stress states around the pile before and after consolidation may be estimated. The final predicted values of remoulded strength and water content of the soil are 28·1 kN/m^2 and 24·3% respectively. These figures compare well with values measured by Eide *et al.* of 27 kN/m^2 (peak strength of 40 kN/m^2) and 24% over three years after installation of the pile, by which time consolidation was presumably complete. The same approximate method of estimating the final strengths and water content of the soil close to the pile may be used as for the Seed and Reese case study. The original excess pore pressure may be estimated as

$$u_{max} = 4 \times c_u(0)_{peak} + \Delta p_{rem}' = 4 \times (20 \times 2/\sqrt{3}) + 2(20-4)/1{\cdot}2 = 119 \text{ kN/m}^2 \qquad (25)$$

The final radial effective stress will then be $(\sqrt{3}/M + 1)c_u(0)_{rem} + 0{\cdot}54 \times 119 = 76$ kN/m^2. For $M = 1{\cdot}2$, the Cam-clay model gives $(c_u/\sigma_c') = 0{\cdot}3$ which leads to an estimate for the final soil strength of 23 kN/m^2. The corresponding water content is 25·3%. Again this approximate

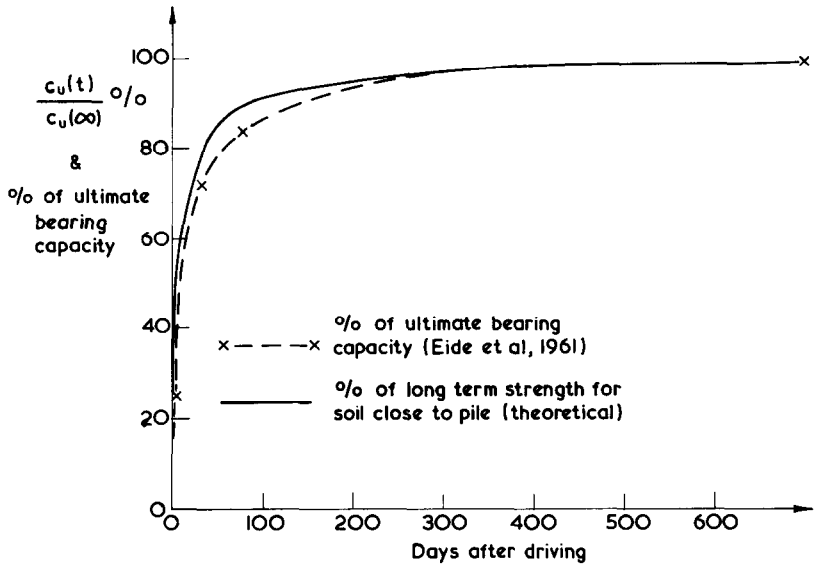

Fig. 24. Comparison of measured increase in bearing capacity of pile with theoretical increase in strength of soil adjacent to pile (data from Eide *et al.*, 1961)

method provides a conservative estimate of the strength gain close to the driven pile. It is interesting to note that the average adhesion down the pile was estimated by Eide *et al.* to be approximately 30 kN/m^2, although there was some doubt as to the final tip capacity since the pile was uninstrumented. (The overall pile capacity was just under 300 kN.) This figure is consistent with the final remoulded soil strength calculated using the finite element method.

Values of the permeability of the Drammen clay were not given, but a value of the coefficient of consolidation has been estimated by Simons (1957) from a study of the settlement records of a building on Drammen clay. Simons gives a figure of $c_v = 3$ m^2/year[3]. From this figure it is possible to estimate a permeability, based on a soil compressibility given by equation (20) and a value for κ of 0·03. This leads to a value for permeability of $k \simeq 2 \times 10^{-10}$ m/s. Taking this value, it is possible to compare the predicted increase in soil strength with the measured increase in pile bearing capacity. This comparison is shown in Fig. 24 where reasonable agreement between the two curves may be observed.

CONCLUSIONS

The formulation of reliable design rules for estimating the shaft capacity of a driven pile has always been hindered by the lack of knowledge of the actual stress state around the pile after installation. By modelling the installation as the expansion of a cylindrical cavity, it has been possible to estimate the effective and total stress changes both during expansion of the cavity and during subsequent consolidation of the soil around the pile. The modified Cam-clay soil model has been used to investigate how the soil behaviour during these processes is affected by the past stress history of the soil.

The most striking feature of the results—which has far-reaching consequences—is that the

[3] Eide *et al.* (1961) quote values of c_v between 1 and 4 m^2/s, which is clearly a typographical error—possibly for m^2/year.

stress changes, normalized by the initial value of the undrained shear strength, are nearly independent of the value of OCR. This would indicate that the shaft capacity of a driven pile in a soil of a given undrained strength is effectively independent of OCR. In terms of the current practice of pile design, it means that the value of α is essentially independent of OCR for a driven pile. This conclusion will not of course apply to bored piles, nor to the values of α relevant to the pile during the consolidation process. The disparity between this result and current design practice (based on experimental evidence) must clearly be the subject of further research.

Simple design rules, in terms of basic soil properties, have been given for estimating the maximum excess pore pressures generated during driving and the times necessary for these pore pressures to dissipate. The final effective stress state close to the pile is one where the minor principal stresses are equal. The radial stress is the major principal stress and the ratio of the vertical and circumferential stresses to the radial stress is close to the natural K_0 for normal one dimensional consolidation. For Boston Blue clay, the final radial effective stress is about 5 times the original undrained shear strength. The undrained shear strength close to the pile increases correspondingly by a factor of about 1·6. For other clay, the factor will vary; preliminary studies have shown ratios of $c_u(\infty)/c_u(0)$ which range from 1·3 at low values of M (or ϕ') up to 2 at high values of M. It is hoped to produce charts relating this factor to relevant soil parameters in another paper.

The concepts of critical state soil mechanics are based on the strength of soil at large strains and are thus particularly relevant to the behaviour of soil close to a driven pile. It has been shown that the Cam-clay soil model not only enables a general picture of the consolidation process to be drawn but also gives good agreement with measurements from field tests on piles in sensitive soils which are otherwise difficult to treat analytically. The rate of increase in pile capacity with time after driving and also the long term changes in strength and water content of the soil close to the pile shaft may be estimated with reasonable accuracy.

The analysis and results presented here are based on conditions of plane strain. Thus shear stresses acting in the r–z plane and out of plane (vertical) movement due, for example, to the presence of the ground surface have both been ignored. The manner in which these factors may affect the conclusions drawn must be the subject of future research. Also, it is necessary to study the changes in effective stress around a pile when it is loaded, and the ratio of the adhesion between pile and soil to the strength of the intact soil for different pile materials (see, for example, Potyondy, 1961). However, it is hoped that straightforward design rules may eventually be formulated incorporating ideas and results contained in this Paper. Such rules should provide considerable improvements to both total and effective stress methods of estimating pile shaft capacity.

ACKNOWLEDGEMENTS

The Soil Mechanics group of the University of Cambridge has an extensive and continuing programme of theoretical and experimental research into the performance of piles and piled foundations. The work reported in this Paper forms part of that programme and was instigated by a contract from the Exxon Production Research Company. The Authors gratefully acknowledge this financial support, and the interest, stimulus and contribution provided by Dr T. W. Miller during the early phases of this work.

REFERENCES

Banerjee, P. K. & Stipho, A. S. (1979). An elastoplastic model for undrained behaviour of heavily overconsolidated clays. *Int. J. Numer. Anal. Methods Geomechanics* 3, No. 1, 97–104.

Bjerrum, L. & Johannessen, I. (1961). Pore pressures resulting from driving piles in soft clay. *Pore pressure and suction in soil.* London: Butterworth

Burland, J. B. (1973). Shaft friction of piles in clay—a simple fundamental approach. *Ground Engng* **6**, No. 3, 30–42.

Butterfield, R. & Banerjee, P. K. (1970). The effect of pore water pressures on the ultimate bearing capacity of driven piles. *Proc. Second South East Asian Conf. Soil Engng, Bangkok*, 385–394.

Carter, J. P., Randolph, M. F. & Wroth, C. P. (1979). Stress and pore pressure changes in clay during and after the expansion of a cylindrical cavity. Unpublished.

Chandler, R. J. (1968). The shaft friction of piles in cohesive soil in terms of effective stress. *Civ. Engng Publ. Wks Rev.* **63**, 48–51.

Clark, J. I. & Meyerhof, G. G. (1972). The behaviour of piles driven in clay. An investigation of soil stress and pore water pressure as related to soil properties. *Can. Geotech. J.* **9**, No. 3, 351–373.

Cooke, R. W. & Price, G. (1973). Strains and displacements around friction piles. *Proc. Eighth Int. Conf. Soil Mech. Edn Engng, Moscow*, **2**, No. 1, 53–60.

Cooke, R. W. (1974). The settlement of friction pile foundations. *Proc. Conf. Tall Buildings, Kuala Lumpar.*

Cummings, E. A., Kerhoff, G. O. & Peck, R. B. (1950). Effect of driving piles in soft clay. *Trans. Am. Soc. Civ. Engrs* **115**, 275.

Eide, O., Hutchinson, J. N. & Landva, A. (1961). Short and long term test loading of a friction pile in clay. *Proc. Fifth Int. Conf. Soil Mech. Fdn Engng, Paris*, 45–54.

Esrig, M. I., Kirby, R. C., Bea, R. G. & Murphy, B. S. (1977). Initial development of a general effective stress method for the prediction of axial capacity for driven piles in clay. *Proc. Offshore Technology Conference, Houston.*

Esrig, M. I. & Kirby, R. C. (1978). Soil capacity for supporting deep foundation members. *American Socity for Testing and Materials Symposium on Behaviour of Deep Foundations, Boston.*

Hill, R. (1950). *The mathematical theory of plasticity.* Oxford University Press.

Kirby, R. C. & Wroth, C. P. (1977). Application of critical state soil mechanics to the prediction of axial capacity for driven piles in clay. *Proc. Offshore Technology Conf., Houston.*

Koizumi, Y. & Ito, K. (1967). Field tests with regard to pile driving and bearing capacity of piled foundations. *Soils Fdns* **7**, No. 3.

Ladanyi, B. (1963). Expansion of a cavity in a saturated clay medium. *J. Soil Mech. Fdn Engng Am. Soc. Civ. Engrs* **89**, SM4, 127–161.

Lo, K. Y. & Stermac, A. G. (1965). Induced pore pressures during pile driving operations. *Proc. Sixth Int. Conf. Soil Mech. Fdn Engng, Montreal* **2**.

McClelland, B. (1972). Design and performance of deep foundations in clay. General Report. *Am. Soc. Civ. Engrs Specialty Conf. Performance of Earth and Earth-supported Structures* **2**, 111–114.

Meyerhof, G. G. (1976). Bearing capacity and settlement of pile foundations. Eleventh Terzaghi Lecture. *J. Geotech. Engng Div. Am. Soc. Civ. Engrs* **102**, GT3, 195–228.

Naylor, D. J. (1975). *Non-linear finite element models for soils.* PhD thesis, University College of Swansea, Wales.

Palmer, A. C. (1972). Undrained plane-strain expansion of a cylindrical cavity in clay: simple interpretation of the pressuremeter test. *Géotechnique* **22**, No. 3, 451–457.

Parry, R. H. G. & Amerasinghe, S. F. (1973). Components of deformation in clay. *Symp. Plasticity Soil Mech., Cambridge*, 108–126.

Parry, R. H. G. & Swain, C. W. (1977a). Effective stress methods of calculating skin friction on driven piles in soft clay. *Ground Engng* **10**, No. 3, 24–26.

Parry, R. H. G. & Swain, C. W. (1977b). A study of skin friction on piles in stiff clay. *Ground Engng* **10**, No. 8, 33–37.

Potyondy, J. G. (1961). Skin friction between various soils and construction materials. *Géotechnique* **11**, No. 4, 339–353.

Randolph, M. F. (1977). *A theoretical study of the performance of piles.* PhD thesis, University of Cambridge, England.

Randolph, M. F., Steenfelt, J. S. & Wroth, C. P. (1979). The effect of pile type on design parameters for driven piles. *Proc. Seventh European Conf. Soil Mech. Fdn Engng* **2**, 107–114.

Randolph, M. F. & Wroth, C. P. (1978). An analytical solution for the consolidation around a driven pile. Unpublished.

Roscoe, K. H. & Burland, J. B. (1968). On the generalized behaviour of 'wet' clay. In *Engineering plasticity* (Heyman, J. and Leckie, F. A., Eds). Cambridge University Press, 535–609.

Roy, M., Michaud, D., Tavenas, F. A., Leroueil, S. & La Rochelle, P. (1975). The interpretation of static cone penetration tests in sensitive clays. *Proc. Eur. Symp. Penetration Testing, Stockholm* **2.1**, 323–331.

Schofield, A. N. & Wroth, C. P. (1968). *Critical state soil mechanics.* New York: McGraw-Hill.

Seed, H. B. & Reese, L. C. (1955). The action of soft clay along friction piles. *Proc. Am. Soc. Civ. Engrs* **81**, Paper 842.

Simons, N. (1957). Settlement studies on two structures in Norway. *Proc. 4th Int. Conf. Soil Mech. Fdn Engng, London* **1**, 431–436.

Skempton, A. W. & Northey, R. D. (1953). The sensitivity of clays. *Géotechnique* **3**, No. 1, 30–53.
Soderberg, L. O. (1962). Consolidation theory applied to foundation pile time effects. *Géotechnique* **12**, No. 3, 217–225.
Terzaghi, K. (1943). *Theoretical soil mechanics*. New York: Wiley.
Tomlinson, M. J. (1957). The adhesion of piles driven in clay soils. *Proc. 4th Int. Conf. Soil Mech. Fdn Engng, London* **2**, 66–71.
Tomlinson, M. J. (1971). Some effects of pile driving on skin friction. *Behaviour of piles*. London: Institution of Civil Engineers, 107–114.
Webb, D. L. (1967). *The mechanical properties of undisturbed samples of London clay and Pierre shale*. PhD thesis, University of London.
Wroth, C. P. (1971). Some aspects of the elastic behaviour of overconsolidated clay. *Stress strain behaviour of soils*. R. H. G. Parry (ed.). Foulis, 347–361.
Wroth, C. P. (1972). Discussion on *Specialty conference on performance of earth and earth-supported structures* **3**, 231–234. New York, American Society of Civil Engineers.
Wroth, C. P. (1977). The predicted performance of a soft clay under a trial embankment loading based on the Cam-clay model. *Finite elements in geomechanics* (G. Gudehus, Ed.). London: Wiley, 191–208.
Wroth, C. P. & Hughes, J. M. O. (1973). An instrument for the insitu measurement of the properties of soft clays. *Proc. 8th Int. Conf. Soil Mech. Fdn Engng, Moscow* **1**, 487–494.
Wroth, C. P. & Simpson, B. (1972). An induced failure at a trail embankment: II. Finite element computations. *Specialty conference on performance of earth and earth-supported structures* **1**, 65–80. New York: American Society of Civil Engineers.
Yudhbir, (1973). Field compressibility of soft sensitive normally consolidated clays. *Géotechnical Engng* **4**, 31–40.
Zienkiewicz, O. C. & Naylor, D. J. (1971). The adaptation of critical state soil mechanics theory for use in finite elements. *Stress Strain Behaviour of Soils. Proc. Roscoe Memorial Symp., Cambridge*. Foulis, 537–547.
Zytynski, M., Randolph, M. F., Nova, R. & Wroth, C. P. (1978). On modelling the unloading-reloading behaviour of soils. *Int. J. Numer. Anal. Methods Geomech.* **2**, No. 1, 87–93.